Exploratory Research on Charged Electrodes for Propulsion

Author:
Matsoukas, George

Publication Date:
2014

DOI:
https://doi.org/10.26190/unsworks/17189

EXPLORATORY RESEARCH ON CHARGED ELECTRODES FOR PROPULSION

By

George Matsoukas

Supervisor N.A. Ahmed

A thesis submitted in partial fulfilment of the requirements for the degree of

Masters by Research

School of Mechanical and Manufacturing Engineering
Department of Aeronautical Engineering
The University of New South Wales
Sydney, Australia

June 2014

This thesis is dedicated to my parents

CERTIFICATE OF ORIGINALITY

I hereby declare that this submission is my own work and to the best of my knowledge it contain no materials previously published or written by another person, nor material which to a substantial extent has been accepted for the award of any other degree or diploma at UNSW or any other educational institution, except where due acknowledgment is made in the thesis. Any contribution made to the research by other, with whom I have worked at UNSW or elsewhere, is explicitly acknowledged in the thesis.

I also declare that the intellectual content of this thesis is the product of my own work, except to the extent that assistance from others in the project's design and conception and linguistic expression is acknowledged.

George MATSOUKAS

____

Name

ACKNOWLEDGEMENT

I would like to express my special appreciation to my supervisor Associate Professor Ahmed. I thank you for encouraging my research and for allowing me to grow as a research student. Your relentless support and understanding have made this thesis possible.

Secondly, I would like to thank my family for their support and guidance throughout my study. I could not have done this without you.

Publications resulting from this thesis

Matsoukas, G., N. A. Ahmed. ‘Experimental investigation of employing asymmetrical electrodes in propulsion of vehicles’, Procedia Engineering 49 (2012): 247-253

Matsoukas, G., Ahmed, N.A., 'Investigation of Ionic Wind as a Means of Generating Propulsive Force', International Review of Aerospace Engineering (IREASE), Praise Worthy Prize S.r.l., Vol. 5 No.2, April 2012, pp 35-39

Matsoukas, G., Ahmed, N.A., ‘Manufacture of Model Apollo Capsule Utilizing Pulsed-Plasma Jet for Bow Shock Dispersion’, Applied Engineering Mechanics, (accepted April 2014)

Matsoukas, G. and Ahmed, N., "Experimental Investigation of Asymmetrical Capacitors for Electric Propulsion," SAE Technical Paper 2014-01-2221, 2014, doi:10.4271/2014-01-2221.

ABSTRACT

The Biefeld-Brown effect has remained a mysterious physical phenomenon for nearly 100 years. It was shown in patents by its discoverer that a force exists between two highly charged electrodes which generally move towards the one of smaller physical dimensions. The system converts electrical energy directly into mechanical force making it attractive for a potentially propulsive application. At current, theories surrounding the effect range from ionic wind to artificial gravity. The research discussed herein investigates the theories surrounding the effect through analyses of the available literature coupled with an experimental program to gain a deeper understanding of the observed force. The experimental program is broken up into two tiers which investigate charged electrodes dependent on both fluid dielectric and solid dielectric mediums. It is drawn from the investigation that there are in fact two independent phenomena which have been attributed to the Biefeld-Brown effect resulting in confusion over the decades. From the fluid dielectric experiments conducted in this study, new insight into ionic wind theory has been made by cross examining collector electrode radius of curvature $\boldsymbol{r_c}$ and separation gap $\boldsymbol{d}$. A maximum effectiveness of $\boldsymbol{\theta = 44.5 mNW^{-1}}$ at thrust $\boldsymbol{T = 2.62 mNm^{-1}}$ was achieved. In addition, it is also shown that magnetic fields enhance the thrust performance that is proportional to voltage input. From the solid dielectric experiments it is deduced that ionic wind is not the cause of the effect, rather, the effect performance is primarily based on the amount of energy stored between the electrodes as well as the ability for the dielectric material to distort the electric field.

TABLE OF CONTENTS

LIST OF FIGURES

LIST OF TABLES

NOMENCLATURE

μ = *ion mobility*

F = *Force on electrodes*

I = *Current*

χ = *Thrust efficiency*

W_k = *Kinetic energy of gas flow*

W_j = *Electric power in discharge*

u = *Neutral gas flow*

V_{drift} = *Ion drift velocity*

T_{MAX} = *Maximum thrust*

E = *Electric field*

V = *Voltage*

d = *Distance between electrodes*

ρ = *Charge density*

V_o = *Corona inception voltage*

C = *Constant depending on electrode geometry*

θ = *Effectiveness*

F_d = *Drag Force*

S = *Surface Area*

C_x = *Drag flow coefficient*

v = *Neutral air velocity*

δ = *Thickness*

η = *Flow efficiency*

RH = *Relative humidity*

L = *Electrode length*

l_c = *Collector electrode depth*

r_c = *Collector electrode radius of curvature*

Φ_w = *Emitter electrode diameter*

Chapter 1 INTRODUCTION

This chapter introduces the subject of investigation, namely, the Biefeld-Brown effect. In addition, the research objectives, scope and structure are explained in detail.

1.1 PROBLEM STATEMENT

Electric propulsion has been a concept of the future for over one hundred years. Potential military, commercial and space applications make the Biefeld-Brown effect an extremely important concept despite being relatively neglected by mainstream science.

Discovered in 1928, the Biefeld-Brown effect was believed to have linked electricity and gravity, which led to the belief that the Biefeld-Brown effect was an anti-gravity phenomenon[1]. As a result, many of the original experiments and work on the effect became classified by the American Army and public interest on the topic ended[2]. More recently, however, certain groups have revived the Biefeld-Brown effect in an attempt to understand its workings and its feasibility as a propulsion device. Conflicting reports on the working mechanism coupled with claims of success of experimental models in vacuum chambers means the effect remains somewhat shrouded in mystery and left for the dissemination by conspiracy theorists.

Essentially, the Biefeld-Brown effect demonstrates that when a high voltage is applied to a pair of electrodes and a leakage current is flowing, a net force is observed in the direction of the positive electrode. However, when the electrodes consist of different physical dimensions, the force is seen to move in the direction of the smaller electrode.

The Biefeld-Brown effect directly converts electric potential energy into mechanical force as well as being relatively easy to construct with simple components. In addition, the system functions with minimised noise and heat signatures. Figure 1 illustrates a simple outline of the Biefeld-Brown whereby the system moves towards the smaller electrode.

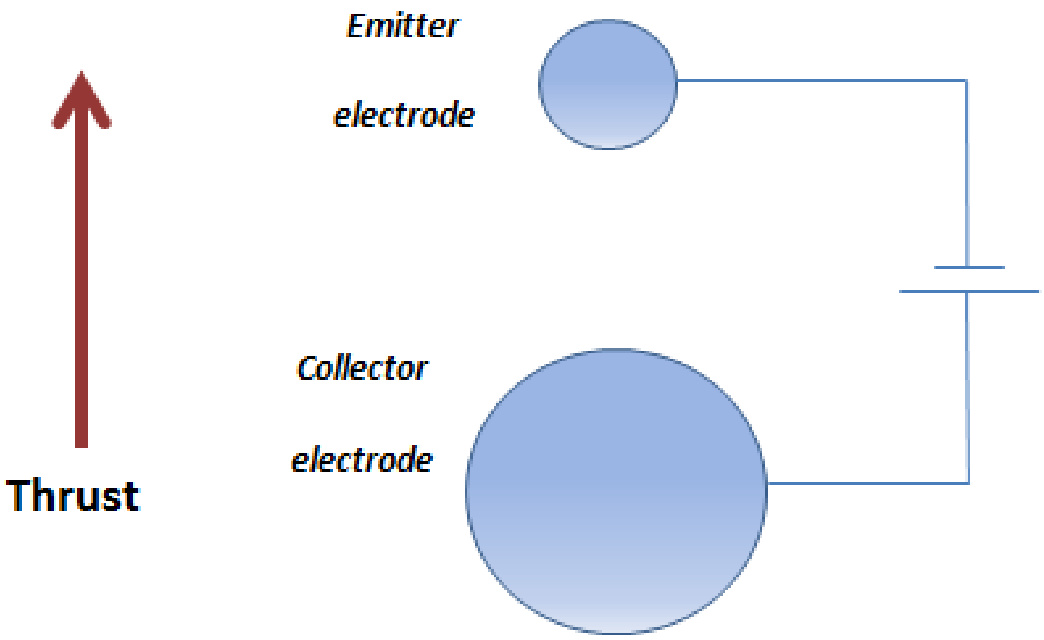

Figure 1 Asymmetrical circuit with Biefeld-Brown force

At this point the effect is yet to be fully explained or fully understood. Varying explanations of the effect and its potential to have practical applications have resulted in a range of different schools of thought on its functionality. Published literature provides explanations which span from ionic wind theories[1, 3] to electro-gravity [4-7] based theories resulting in the generation of artificial gravity.

1.2 OBJECTIVE

The primary focus of this research thesis is broken up into three main components.

- Firstly, this thesis aims to analyse the available literature surrounding the Biefeld-Brown effect in order to derive a thorough understanding of the phenomenon. This is also to be conducted in an attempt to provide insight into the mystery which surrounds the cause of the observed force.

- The second aim of this thesis is to engage into an experimental program which will understand the physical characteristics that govern the creation of thrust on highly charged electrodes. These experiments will focus on testing current theories surrounding the effect as well as testing and analysing the primary parameters of the phenomenon. To this end, it is hoped a definitive explanation may be put forward to end the effects' ambiguity.

- The third primary objective is to optimise and enhance the performance and efficiency of the effect. In addition, a greater understanding of the characteristics which constitute the production of wind may potentially lead to practical applications in areas of electric propulsion, active flow control and ionic fans for computer circuitry in laptops. In order to achieve the above goals, several models will be constructed and tested.

Within the scope of the two primary aims of the thesis, this thesis also aims to:

- Inform the reader of the physics and discovery behind the Biefeld-Brown effect and also current research in this topic area.

- Provide examples and explanations of current theories on the Biefeld-Brown effect.

- Present the design and the processes involved in constructing and testing model craft consisting of highly charged electrodes.
- Provide results and conclusions which address the thesis aims.

1.3 RESEARCH SCOPE

During the course of this research, a series of models are constructed and tested focusing on two main areas investigation. Firstly, tests were conducted to understand the effects of extreme asymmetry of electrodes utilising a fluid dielectric medium i.e. air. The basis behind these experiments was to ionize the surrounding air to conform to ionic wind theories. The second focus of the research, however, consists of a set of experiments which utilize copper electrode plates charged to high voltages which are enhanced with solid dielectric materials. These set of experiments do not ionize the air and aim to understand the force on the electrodes in terms of a non- ionic wind explanation.

1.4 STRUCTURE OF THIS THESIS

This thesis will begin with the discoveries and inventions of Thomas Townsend Brown from which the Biefeld-Brown effect stems. Following this analysis of the original documents, a review of the available research on the Biefeld-Brown effect will be conducted which is split into two categories. The first will discuss the research conducted towards an ionic-wind explanation of the effect. To this end, a deeper understanding of the physics behind electro-hydrodynamics (EHD) is sought to provide insight and validity to this theory in explaining the Biefeld-Brown effect. The second half of Chapter 2 discusses research which has been conducted which concludes that the Biefeld-Brown effect is not the result of EHD but rather relying on some other unknown principles. Chapter 2 is then concluded with an explanation of the underlying principles of EHD theory as well as some alternative explanations.

Chapter 3 is the first of two experimental investigations which aims to fulfil the thesis objectives. Namely, this experimental program is designed to experiment extremely asymmetric electrodes charged to high voltages in a fluid dielectric medium i.e. air in order to test and validate the ionic wind theory. In sight of this, a theoretical model which describes the force on charged electrodes is provided and used as a benchmark for the experimental program. A series of experiments are conducted which test various geometric variables of the system for an enhanced understanding. Chapter 3 concludes with several novel experiments which result in enhanced thrust and efficiency levels.

Chapter 4 outlines the second experimental investigation which is conducted to investigate the observed force on charged plates that do not require the ionization of a fluid dielectric medium. To this end, a series of experiments are performed which aim to gain a deeper understanding to the cause behind the observed thrust and the effect of solid dielectric materials on the thrust enhancement.

Finally, discussions of the results gained in this research are provided in Chapter 5 followed by conclusions.

Chapter 2 LITERATURE REVIEW

Provided herein is an account of the history of the force observed on asymmetrical capacitors since its discovery in the 1920's.

Following the discovery and research conducted by its discoverer, two schools of thought have arisen which provide explanations for the effect. The first being an ionic wind explanation is covered in detail from its first research to current times. The second consists of several alternate researches which may best be attributed to a field described as non-ionic wind.

In addition, analyses of several major conventional theories are also provided.

2.1 BIEFELD-BROWN EFFECT

2.1.1 Background

The struggle to combine electromagnetism with the relatively weak yet universal force of gravitation is a task yet to be accomplished. However, in the early 1920's, claims for one such link arose through the findings of Thomas Townsend Brown. Brown, still a student, was experimenting with 'Coolidge tubes', invented in 1913 by American physical chemist William D. Coolidge, when he observed an anomalous force on the tubes charged to high voltages. Believing he had discovered a potentially new field of physics, Brown addressed many of his physics teachers and professors only to be shut down and ignored. After some time, Brown eagerly acquainted himself with a professor in physics, Paul Alfred Biefeld, who had noticed the same anomalous force with charged electrodes. Brown continued his research on high voltage electrodes while he was in graduate school under the supervision of Biefeld. The corroboration between the two led to the coining of the term, the Biefeld-Brown effect.

The first publicized research came in the form of Browns first patent[8] issued on November 1928, titled, *A Method of and an Apparatus or Machine for Producing Force or Motion*. It is expressed through this patent that Brown believed he had discovered the coupling characteristic between electricity with gravity and essentially discovered a means to control it. Brown provides a series of diagrams and drawings which illustrate a force observed on oppositely charged electrodes from negative to positive. Furthermore, there is no mention of asymmetry between electrodes, rather, Brown accounts for the force as a distortion of the local gravitational field through the aggregation of electrical charge.

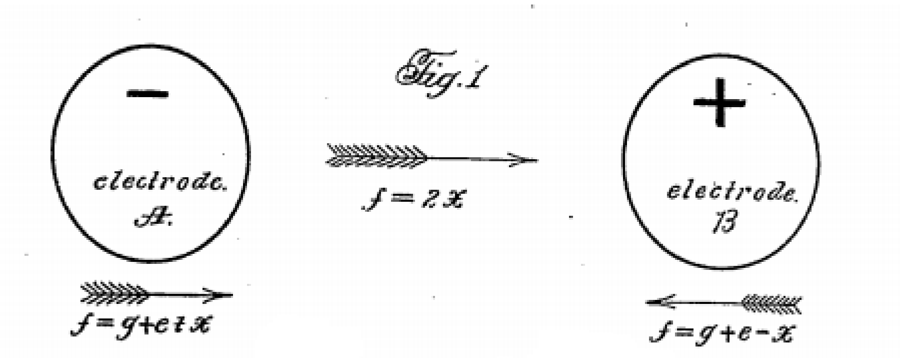

Figure 2 Browns' Ꭓ-force between charged electrodes[8]

One such diagram provided in the patent, shown in Figure 2, illustrates a force which moves toward the positive electrode by a function of 2Ꭓ, where Ꭓ is the force due to unbalanced gravitational forces caused by excess charge on electrode.

Here brown equates the force on electrodes A and B as,

$$F_a = g + e + \text{Ꭓ} \tag{1}$$

$$F_b = g + e - \text{Ꭓ} \tag{2}$$

Solving simultaneously we get,

$$F_T = 2\cancel{X} \tag{3}$$

in the direction of A to B.

Brown also makes characterization observations, noting that to optimise the effect; the insulation between electrodes must have the smallest distance possible, although consisting of the highest puncture voltage. In addition, he makes note that the potential difference must be as high as possible with as many plates as possible for maximum effect. An important observation is, however, that once the voltage reaches a certain point, named the 'saturation voltage' by Brown, there is a reversal in the direction of force; this should be avoided. It is also disclosed within this patent that there exists a force between an anode and cathode in a vacated chamber insinuating that the effect is entirely dependent on a gravitational field to exist. More elaborate patent diagrams show an electrostatic motor which Brown claims to be self-sustaining by drawing energy from the surrounding gravitational field; a device which can run itself and provide excess energy. However, there was a lack of experimental evidence and thorough understanding of concepts like electromagnetism and gravity for such claims to be taken seriously[1, 9].

It is only through Browns next patent[10] issued in 1960 titled *Electrokinetic Apparatus*, that a different understanding of the effect was provided. In this patent, Brown introduces the concept of asymmetry between the electrodes and moves away from an electro-gravity explanation, describing the phenomenon in terms of dielectric movement. One such patent claim suggests that when charged electrodes are fixed in relation to each other and immersed in a dielectric fluid medium, they experience a force through the medium with respect to the dielectric material. Alternatively, if the electrodes are fixed with respect to the surrounding medium, the fluid dielectric moves away from the smaller electrode towards the larger electrode like a fan pushing wind. The major difference in this patent from the first is the dependence on a fluid dielectric medium for the effect to function.

Another feature expressed in this patent is that the force on an asymmetrical capacitor has the potential for vehicle propulsion. Here, Brown makes note of the superiority of his system over conventional methods to convert electricity to mechanical force. Brown outlines the elimination of moving parts and intermediate machinery to convert the energy. In addition, he expresses the saving in costs of parts and maintenance as well as its relatively light weight and small design. In his experiments, Brown claims that his model asymmetrical thrusters shown in Figure 3managed to travel 17ft/s in circular motion, utilising 50kV. These devices show a large flat electrode made of aluminium and a small electrode, usually wire, which are charged to high voltages of different polarity. Brown makes reference to the generation of ion wind and projected ions and the possibility that this is the cause of the thrust. It is this basic configuration which is now commonly referred to as a 'lifter' and commonly experimented with amongst researchers today. The experiments conducted in Chapter 3 will also mimic this original design.

In 1962 Brown was granted another patent[11] titled, *Electrokinetic Transducer*. This patent dealt with Browns findings on an inverse effect to his discovery, i.e. where dielectric medium was made to move between the electrodes, a change in the voltage was observed. This displays similarities to faradays law of induction in relation to electricity and magnetism.

The most important aspect of this new technology is to not only understand its cause, but also to grasp its ability to be utilised as space propulsion. Such an application would require the effect to function effectively in a vacuum. This particular attribute forms the basis of Browns next patent, despite yielding contradictory views on its experimental accuracy.

Issued in 1965 titled, *Electrokinetic Apparatus*, this patent [12] now reverts back to the conclusions expressed in Browns first patent issued in 1928. Essentially, this more recent patent outlines the ability of the effect to be function in a vacuum whereby the thrust force was not reduced to zero despite the removal of all environmental bodies beyond the effective electric field range. This means that this phenomenon does not depend on the ionization of a fluid dielectric medium to generate thrust as expressed in Browns earlier 1960 patent.

FIG. 6

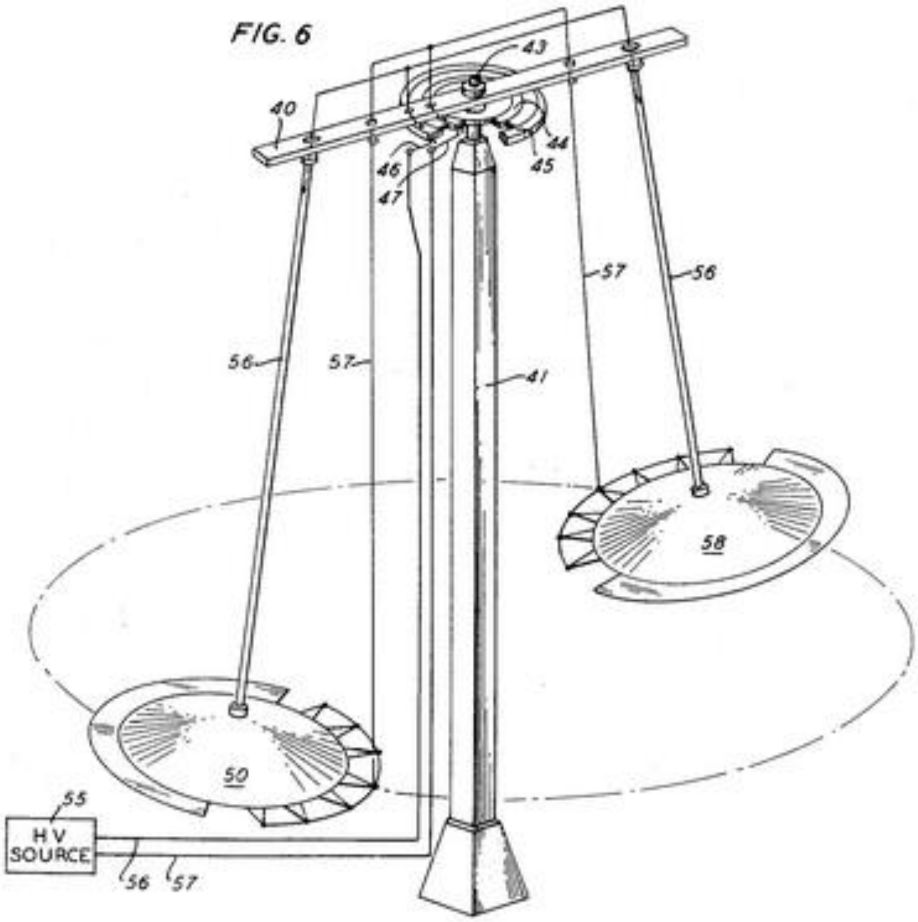

Figure 3 Asymmetrical thrusters rotating around central column[10]

Brown asserts that this is achieved by utilising a shaped electric field to propel a device relative to its surroundings. Brown observes that a reaction force is observed on any material near the device, even through a vacuum to the chamber walls. Brown finds that the thrust is in the direction of high electric flux density to low flux density; the opposite direction to ionic wind devices. This patent also makes note that thrust is produced toward the larger electrode, preferably of an arcuate surface as shown in Figure 4.Thrust is still observed on a single surface, although it is magnified with the presence of another electrode of a smaller, sharper shape.

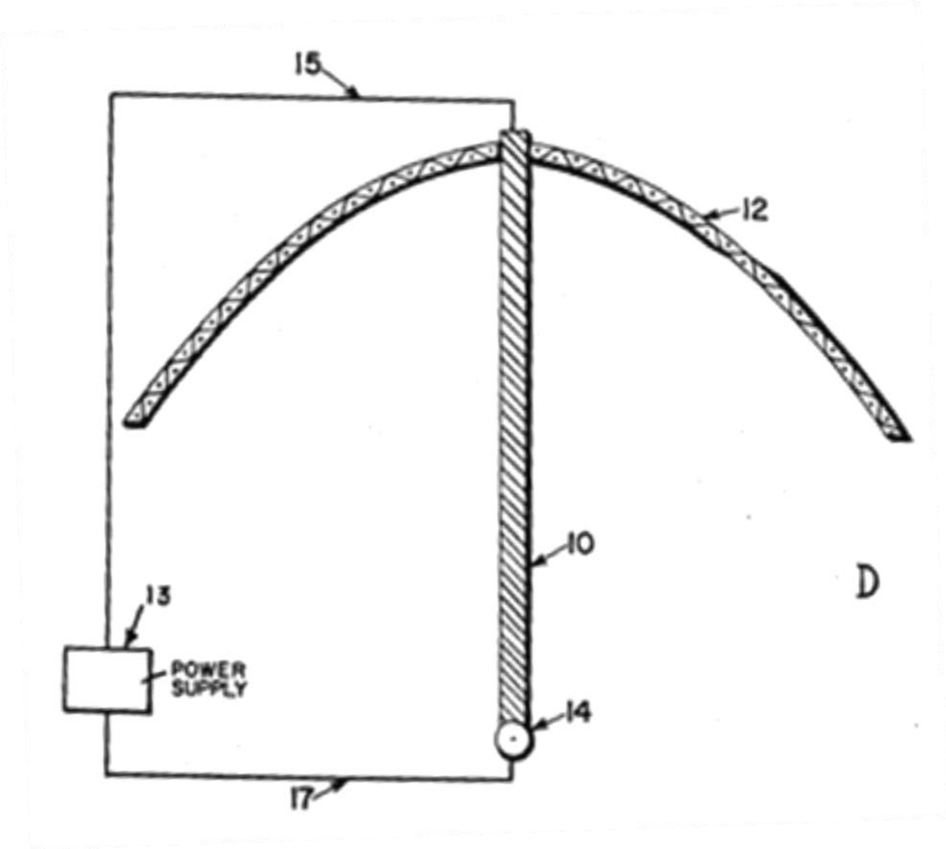

Figure 4 Browns' asymmetric thruster[12]

It is emphasised in this patent that the foundation of the force is in the asymmetry of the electric field, this asymmetry is affected by certain variables. Such parameters for inducing an asymmetric electric field between the electrodes include:

- Physically changing the electrode dimensions creating an unequal electric flux density.
- Changing the mass of dielectric between the electrodes to have more mass at one electrode than the other.

- Changing the density of the dielectric material or changing the dielectric material itself to be denser at one electrode than the other.
- Changing the dielectric strength, electrical or thermal permittivity's of the dielectric material to be more intense at one electrode than the other.

Fundamentally, the patent deals with shaping the electric field to produce force. By achieving an asymmetrical electric field, Brown believed he could generate a reactionless electrostatic force on the electrodes. This is further enhanced by stacking or layering the dielectric material as shown in Figure 5.

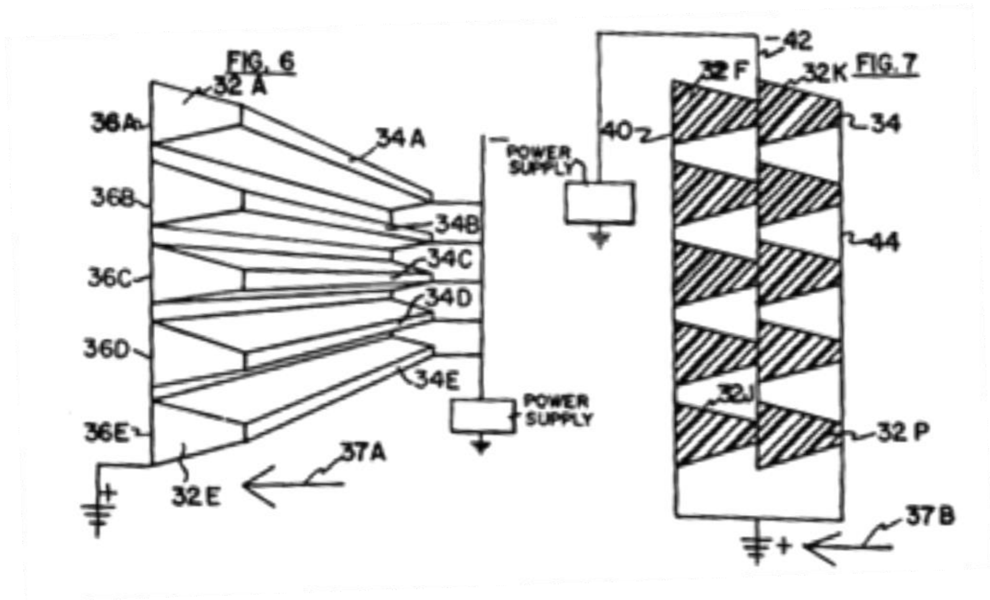

Figure 5 Shaped dielectric and stacked dielectric to enhance weight loss[12]

Essentially, we are now provided with a patent which describes the observed force as an electrostatic force enhanced by an asymmetric electric field. This differs from the previous patents which require a fluid dielectric medium to function. On the contrary, these electrostatic observations are shown to be further enhanced through asymmetry of the solid dielectric material separating the plates.

It can be seen from the patents produced by Brown that the underlying principles governing charged electrodes is rather ambiguous. This ambiguity has resulted in conflict over the explanation of the observed thrust for decades to follow. The subsequent sections aim to review the available literature which has emerged after Browns' discoveries. Appropriately, this is broken into two streams of research. The first will look into the publications which are in support of an ionic wind theory utilising EHD principles. The second will look at any other possible explanations and studies that have emerged contrary to ion wind.

2.1.2 Ion wind developments

The first notable re-creation on the work of Thomas Townsend Browns asymmetrical capacitors came in the form of model 'lifters' by Alexander De Seversky in the early 1960's. De Seversky, who coined the term 'Ionocraft', was the first to reproduce experiments which involved asymmetrical electrodes for propulsion. De Severskys' Ionocraft consisted of combining a series of wires acting as the small electrode, to a mesh plate, acting as the large electrode - charged to high voltages. His experiments managed to make the front cover of popular *Mechanics* magazine[13] in August 1964.The article claimed that the technology was viable over a wide range of speeds, matching those of even jet propulsion. Referenced as a 'magic carpet' it was also claimed to be more efficient that conventional propulsion methods and operational to altitudes of up to almost 100 kilometres. De Seversky and his team at this point, however, had only built small scale models of their Ionocraft out of balsa wood, aluminium wire configurations for the electrodes and a high voltage power supply as shown in Figure 6. Maximum results possible took 90W of power (30kV, 3mA) to lift 57g[14].

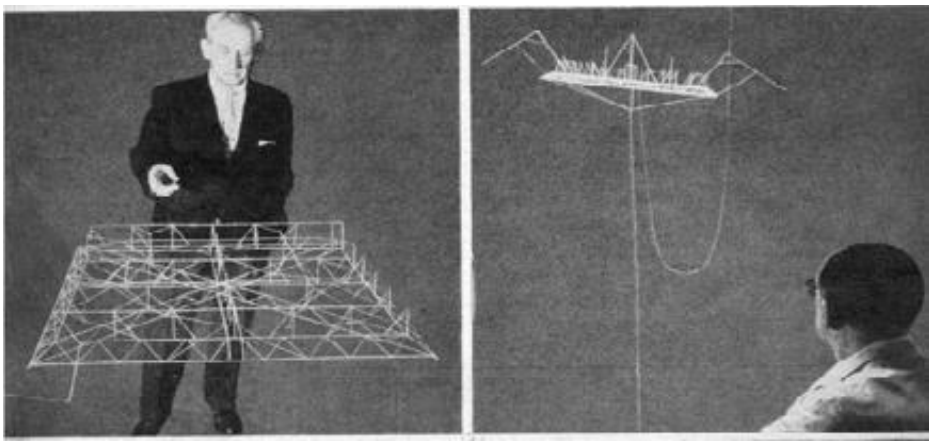

Figure 6 De Seversky demonstrating his model Ionocraft[13]

Observing that the device generated a downward force wind, De Seversky emphasised that this technology is not suitable for space and was designed to work within the atmosphere. De Seversky also reports discordantly with Brown that the thrust efficiency is varied with humidity and air pressure [1], characteristics which may only be attributed to atmospheric functioning.

De Seversky managed to patent his Ionocraft lifters in 1964 in a patent[15] titled, *Ionocraft*.The patent explicitly states De Severskys' understanding of the craft to be the result of ionic wind projecting from the emitter electrode. In fact De Seversky believed the Ionocraft would have extremely high altitude capabilities in the range of 90kms above sea level comparing it to helicopters which only reach approximately 6kms[13].

As a result of this research by De Seversky, the discoveries made by Brown were linked to the field of electro-hydrodynamics (EHD). It was from this link which emerged the ionic wind theory used to explain the anomalous force between asymmetrical electrodes.

Following soon after the claims of De Seversky, ion wind theory was further propelled by the more theoretical works of Cheng in 1962 [16] and Christenson and Moller in 1967[17].Both sets of research investigated the generated thrust by a corona discharge in an air dielectric medium from a highly charged source.

Cheng completed an intense study on ionic wind a possible propulsion system which made three significant conclusions on the performance of EHD propulsion. Firstly it was observed that larger thrust can be achieved more economically by increasing the electrode area rather than by operating in the abnormal glow region. Although, higher thrust is achieved with respect to area it will result in higher specific power consumption. Cheng concludes that the optimum operating level should within the normal glow region across the entire emitter electrode. This correlates to a similar observation by Brown who observed that the formation of a visible corona was unnecessary and even inefficient due to losses in heat and radiation such as visible light.

The second conclusion indicates that for the same amount of thrust, the discharge current density of the corona and consequently the power consumption may be reduced by using gases with larger ion mass and smaller saturation ionization constants. Basically, this means smaller ion mobility μ results in a reduced current discharge for a particular thrust. Lastly, it is concluded that the thrust and the discharge current increase with the square of the gas pressure which provides insight into the potential of the system at high altitudes.

Another serious investigation into corona discharge propulsion was conducted by Christenson and Moller who like Cheng who also developed a 1-D model of an EHD thruster system which was now also compared experimentally. The model was conceived using Navier-Stokes equations and was in compliance with current output for corona discharges. The experimental setup constituted of sharp pointed aluminium rods mounted in plexiglass for the emitter electrode and concentric aluminium rings spanning 0.3557m for the ion collecting electrode. Experimental results achieved thruster efficiency about one half of the values predicted by their model. Christenson and Moller concluded that approximately 90% of the input energy is lost in the form of heat. It was concluded that reducing the ion mobility $\mu$of air molecules by at least 2 orders of magnitude is necessary for practical applications resulting in a competitive efficiency level of approximately 30%.

Similar work conducted by Robinson[18] in the early 1960's also concluded, like Christenson and Moller, that the energy conversion rate of EHD systems is relatively low. Robinson also noted that the production of secondary gases such as ozone in corona discharge can be a significant setback for EHD blowers. Although, in 1986 Bondar and Bastien[19]showed, that the efficiency increases with fluid velocity in their analytical model. They attained experimental results of a conversion efficiency of up to 7.5% by operating with an incoming flow velocity of 50m/s.

Up to this point, an ionic wind theory to explain the Biefeld-Brown effect seemed rather conclusive. However, a research contracted by the Air Force Astronautics Laboratory in 1988 solidified the explanation. Robert Talley [20] of Veritay Technology conducted the first vacuum tests since the claims made in Browns' patent. The report performed many experiments on asymmetrical electrodes similar to those of Brown by suspending them from a thin wire in a vacuum chamber up to 10^{-6}Torr. This allowed for extremely small movements to be detected. Slight movement was observed in the vacuum chamber experiment; this has been explained by Talley as movement due to electrostatic interaction between the thruster and the chamber walls. In addition, there was observed a force during electrical breakdown between the electrodes. However, no explanation for this is given.

Due to the results of Talley, research into the Biefeld-Brown effect diminished for several years as did the hopes of finally linking gravity with electricity and magnetism. However, new interest into efficient electric propulsion systems sparked by NASA reinvigorated research back into the field.

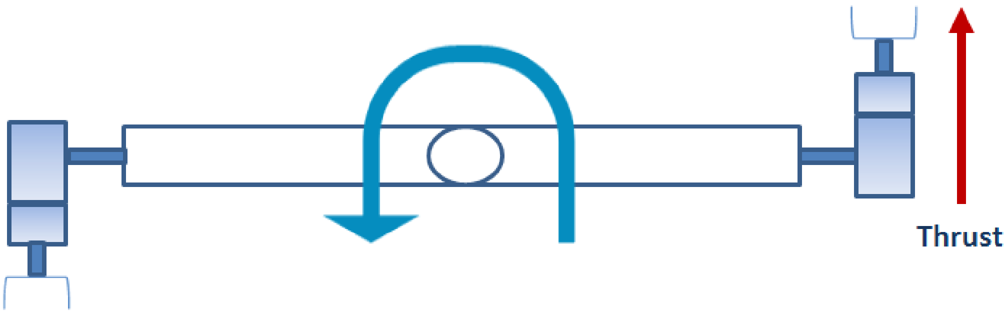

Figure 7 Asymmetrical Capacitor Thrusters rotating around central column

As a result a research was conducted by Campbell of NASA's Marshal Space Flight Centre which designed and tested asymmetrical capacitor thrusters. Asymmetrical thrusters differ slightly to the 'lifters' utilised by and others[9, 21]. Asymmetrical capacitor thrusters consist of a small disk or ring, acting as the small electrode, followed by a hollow cylinder acting as the large electrode. The configuration commonly consists of two asymmetrical thrusters which rotate about a central column. A basic setup of the test rig used by Campbell is shown in Figure 7.

Research into the claims of Brown conducted by Tajmar in 2004 [1] inevitably led, as he believes, to be a misinterpretation of ion wind. Tajmar conducted experiments with asymmetrical electrodes setups similar to those of both Brown[10] and Christenson and Moller[17]. In both setups the asymmetrical electrodes were mounted to a box which acted as a Faraday cage and was grounded. It was intended that any movement made by the asymmetrical electrodes would result in movement on the box, both of which could swing freely. Movements on the box were measured using a laser displacement meter of a sensitivity of $\pm 0.1 \mu m$. Once 38kV was applied to the experimental rig, Tajmar measured oscillations on the box which he believes was a result of corona wind circulation. The derivation of this conclusion was based on the fact that the box always oscillated around the same mean position and that no noticeable linear thrust was observed. Tajmar concludes that even if a possible linear thrust existed, its measurement must have been less that $10 \mu N$ which derives a thrust to power ratio of ${}^{P}/_{F} \geq 2280 WmN^{-1}$. Considering conventional electric propulsion systems range from 20-70 W/mN, this method would be far inferior.

Later on in the same year another investigation into the force on asymmetrical electrodes was conducted by Canning et al[22], contracted by NASA. The Biefeld-Brown effect was addressed and a theoretical and experimental investigation was conducted to determine the cause of the thrust. Within the research several theoretical analyses were provided for possible theories surrounding the effect. Canning et al found that possible thrust due to ablative material on the smaller electrode couldn't be the cause; results showed that a wire of 0.005kg would be completely ablated 10 times over in 1 hour of testing. Although reports from some researches [23] experiencing ablation of the emitter electrode, this was not the cause of thrust.

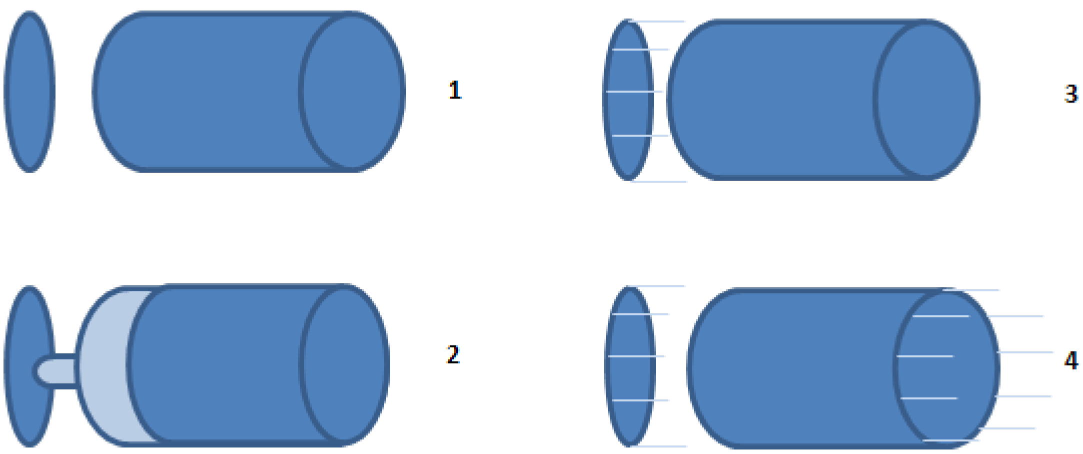

Figure 8 Experimental Asymmetric Thruster Model used by Canning et al

Experiments were conducted on asymmetrical thrusters on a range of different configurations and polarities with the small electrode as a disk rather than a ring. Device 1 consisted only of a disk and a cylinder made of copper. Device 2 is essentially the same configuration however this model also consisted of a small cylindrical solid dielectric material aimed to determine the effect this would have on thrust. Devices 3 and 4 again consist of the same configurations; however, they aim to increase the asymmetry of the electrodes by adding a curvature to the cylinder as well as small aluminium wires to the emitter electrode in device 3 and to both electrodes in device 4.The four models used for experimentation by Canning et al as shown in Figure 8 were tested in different vacuum levels as well as pure Argon and pure Nitrogen. Reduced thrust was achieved in all cases compared to standard pressure air.

Results indicate that generally all the devices moved in the direction of the smaller electrode which is consistent ion wind theory however, in terms of polarity; movement was away from the grounded electrode. In addition, it was seen that circuit 4 moved the fastest due to its enhanced asymmetry. This is suggested to be the result of both the wires which emanate from the electrodes and also the larger radius of curvature on the end of the cylinder. All devices moved faster when the cylinder was grounded and the disk charged. In addition, it was seen that Device 4 moved fastest when the disk was negative, with other devices moving faster when it was positive. No explanation is given for this. However, ion wind as the sole cause of thrust which was further supported with vacuum tests. All the thrusters rotated more slowly as the pressure dropped whereby no movement was seen by any of the thrusters below 300 Torr. There was one exception, thruster 2, whose electrodes were separated by a gap and dielectric material, made 1/8th of a rotation at a pressure of 5.5 x 10-5Torr after an arc formed at 44kV. This is strikingly similar to the result obtained by Talley; however, this motion is not considered the result of the Biefeld-Brown effect but rather the effects of currents in divergent electric fields in 5-D theories which couple the gravitational and electromagnetic fields [4]. Hence, Canning et al conclude from their experimental investigation that the drift of ions colliding with neutral air molecules can be the only explanation.

A more theoretical research produced by Ianconescu et al derives the levitation due to ion wind of their model lifter. This model which was also confirmed by experimental results, accurately describes the force both in respect to current and voltage. By applying the force to current ratio, found experimentally to be 179.72 $NA^{-1}$and understanding that this relationship is based on the distance between the electrodes, Ianconescu et al concludes that,

$$F = \frac{I(1.284b)}{\mu} \tag{4}$$

sufficiently describes the force on asymmetrical capacitors for a positive corona. A more recent extension of previous work, in particular the model derived by Christenson and Moller, is conducted by Pekker and Young in 2011[14]. However, Pekker and Young make note that a significant difference of their model is that it accounts for the dependency of ion mobility on neutral gas density. Hence, a 1-D model of an ideal EHD thruster is deduced for calculating thrust efficiency and maximum thrust of EHD thrusters. It is shown that thrust efficiency equals the ratio of kinetic energy of the gas flow to the electrical power deposited in the discharge. This is directly related to the ratio between neutral gas flow$u$ and ion drift velocity V_{drift} such that,

$$\chi = \frac{W_k}{W_j} \approx \frac{u}{V_{drift}} \tag{5}$$

However, it can be seen from the maximum thrust equation,

$$T_{MAX} \approx \frac{j_{max} \cdot L}{\mu_i} = \frac{9 \cdot \varepsilon_0 U^2}{8 \cdot L^2} \tag{6}$$

that the maximum thrust is independent of ion mobility when$V_{drift} \gg u$. Hence, it is deduced that the increasing of current on the EHD system results in an increase of T_{MAX} and a decrease in thrust efficiency χ. Hence, high thrust and high efficiency are not feasible simultaneously. Pekker and Young also conclude that the performance of EHD thrusters at high altitudes is not practicable due to a rapid increase in ion mobility with elevation; altitudes greater than 5km are deemed unrealistic. As a result of these findings Pekker and Young conclude that a future of an ion wind type system for a thruster application is rather improbable.

Although it has been shown that the ion wind theory is adequately describes the Biefeld-Brown effect, it has resulted in concerns surrounding the limitations on EHD thrusters deeming the efficiency levels inappropriate for propulsive purposes. Majority of the recent research has moved towards increasing this efficiency by investigating and experimenting with certain variables.

One such research conducted by Matsuyama and Barrett in 2013[24] obtained thrust to power ratios believed to be competitive with conventional propulsion technologies. This was shown both theoretically and experimentally whereby thrust to power ratios as high as 100N kW^{-1} was achieved. Matsuyama and Barrett make note that the appropriate metric for the efficiency of ion wind devices is thrust per unit power and not propulsive efficiency (which in this case is zero) or kinetic energy in the exhaust stream which is in this case deemed wasted energy. Both single-stage (SS) and dual-stage (DS) thrusters are experimented.

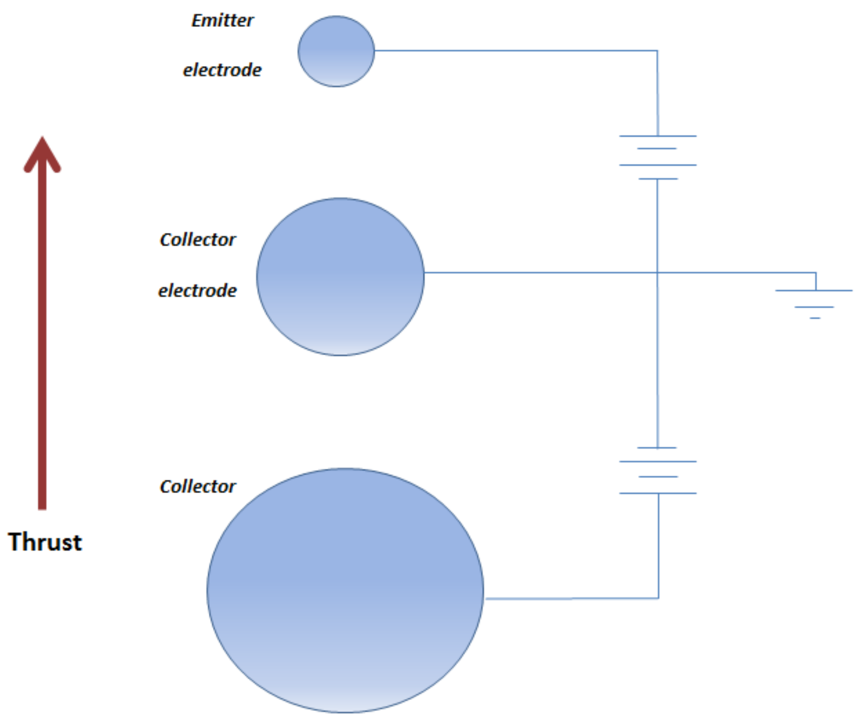

Figure 9 Dual Stage thruster

It is first observed from the SS experiments that no thrust is generated below the inception voltage. Lower levels of thrust versus voltage were observed for greater gap lengths, however, this reversed after gap lengths of 90mm. This variation in thrust performance is correlated to unexplained performance degradation at larger values of current. Masuyama and Barrett hypothesize a second corona is generated near the surface of the collector electrode resulting in degraded performance which they term 'bilinear performance degradation'. Hence, DS thruster configurations as shown Figure 9 involve a third intermediate grounded electrode collinear with the emitter and collector which overcome this drawback. A 1-D model for dual stage thrusters is developed and compared with experimental data which shows that it is likely more efficient than conventional propulsion methods. It is concluded that the thrust of a DS thruster is comparable to modern jet engines at thrust to power ratios of $\eta = 50\%$.

An additional study, concerning the characterization of corona wind for enhanced performance is conducted by Ieta et al in 2013 [25] which varies the amount of asymmetric electrode cells within the system. Ieta et al experimented with the effect of increasing electrode cells as well as changing the distance between the cells to understand the flow dynamics more intricately. Results show that as cell separation increased thrust also increased. Experimenting from 10mm-60mm, 60mm separation provided the greatest results. The experiments however at this point, weren't able to expand the distance any further to determine whether this trend would continue. The second result obtained, showed that the more cells in place resulted in greater thrust. It was shown that the thrust increased fairly linearly with cell modules. However, the thrust per cell was seen to decrease with each new cell added. Although, the sixth cell added went against this pattern. Unfortunately, no further cells could be added to restrictions in the experimental apparatus.

Another study conducted by Primas et al in 2012[21] determines the effect of heating the small electrode on thrust measurements. Primas et al proposes that heating the small electrode should in fact result in greater thrust levels with the same amount of voltage if ion wind is the cause of the thrust. This is attributed to the fact that increased heat will result in the ionization of the surrounding air much faster and with a lower voltage input. By passing a current through the small electrode of their setup it was observed that more than double the thrust was achieved by passing up to 2A of current through the small electrode wire. Primas et al concludes from this that ion wind must be the sole cause of the observed thrust.

Additional research which aims to understand and enhance EHD thrusters through certain variables will be discussed in Chapter 3 as a comparison to the experiments conducted in this thesis.

2.1.3 Non Ionic Wind Developments

Despite the wide range of literature on EHD forces and the wind produced from corona discharges, the question still arises; does this explain in full the force observed on asymmetrical electrodes as described by Brown. As discussed in section 2.1.2, majority of research into the Biefeld-Brown effect has deduced that ion wind is the sole cause behind the observed thrust. However, alternative research has found that there is in fact more to the effects cause than EHD principles. An early research published in *Nature* by Erwin Saxl in 1964[26] describes the unusual effect that high voltages have on the motion of bodies. The intense study was conducted on an electrically charged torque pendulum suspended by an isoelastic wire in a faraday cage, similar to the setup shown in Figure 10.Thousands of tests were conducted over a period of ten years which eliminated as many possible deterring variables such as seisms, micro-seisms, changes in the earth's magnetic flux, temperature, barometric pressure, humidity and other ambient effects. Results from the experiments showed that electric charges impressed on a torque pendulum resulted in period delays. A positive charge caused the pendulum to rotate slower than a negatively charged plate, with an uncharged plate moving the fastest.

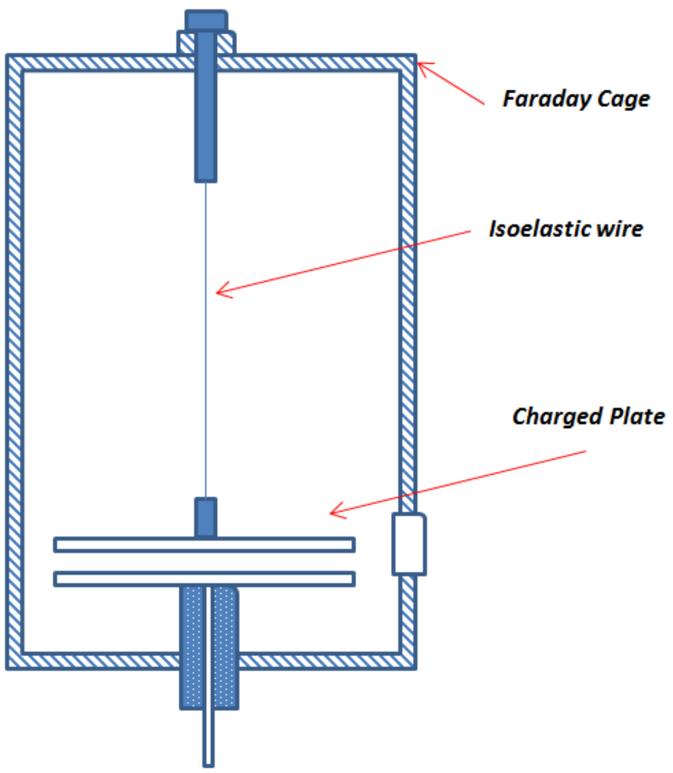

Figure 10 Experimental Setup similar to Saxl

It was deduced that the pendulum period follows a square law with respect to input voltage as shown in Figure 11. In addition, it was noticed that the influence of the voltage on the plate varied with seasonal as well as diurnal variations, a condition also expressed by Brown [27]. Saxl also notes that unusual variations occur during solar and lunar eclipses; aspects which all indicate variations with the earth's gravitational field. Saxl concludes that although he hesitates to provide an explanation of the phenomenon he must suggest, although reluctantly, that there must exist a variation in the local gravitational field of the charged plate. It must be noted however, that more recent reproductions of the same experiments found null results [28].

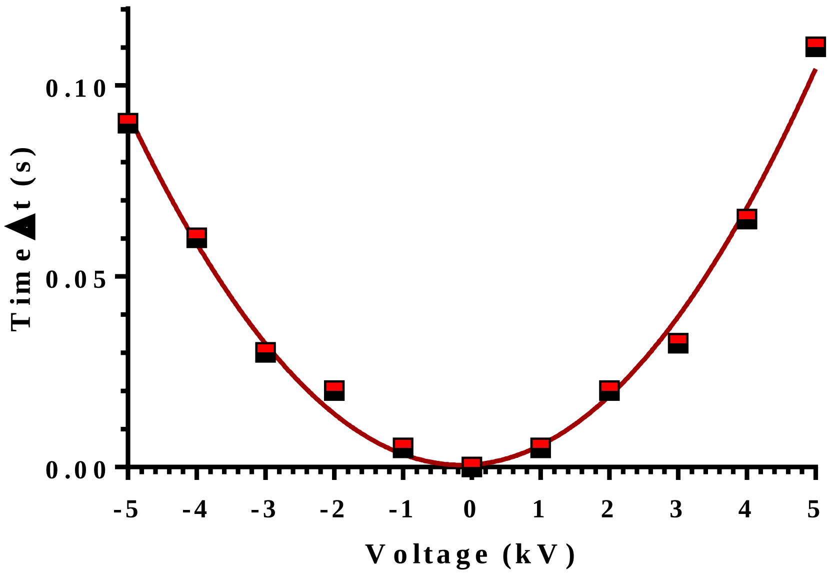

Figure 11 Voltage Vs Time Delay of Charged Plate

Bahder and Fazi in 2002 [9] conducted an analysis of ion wind theories only to conclude that this is not the sole cause of the observed thrust. The ion wind explanation is disregarded because the theoretical results are several orders of magnitude too small to be accepted. Although the theoretical analysis of ion drift theory does match experimental results, the estimates reached are only scaling estimates and would not be applicable to a macroscopic model. Hence, Bahder and Fazi deduce that movement of wind due to ionic effects cannot solely explain the effect. Experiments were conducted on model ‘lifters’ which consisted of wire and aluminium foil as the electrodes. Bahder and Fazi found that the force on the capacitor always tended towards the smaller electrode, independent of the orientation and irrespective of the earth’s surface. As a result, a new thermodynamic theory was proposed based on the polarizability of the fluid dielectric medium.

A key feature not fully explored by many researchers into the force observed on asymmetrical electrodes, is the effect that solid dielectrics have on the observed thrust on charged electrodes. This particular characteristic, although expressed by Brown[12], is often overlooked by proponents of the ionic wind theory. In order to fully understand the anomalous force on charged electrodes, this needs to be taken into account. One such investigation incorporating solid dielectrics and perhaps the most significant research into the force on exhibited on charged electrodes was conducted by Buehler in 2004[29].

Buehler makes an intense experimental investigation on the force on single and parallel plates charged between 100-200kV. Measurements are taken with respect to the earth’s gravitational, magnetic and electric fields to determine any possible relationship. Firstly, from the single charged plate experiments, the charged plate continued to reduce in weight despite the electric polarity orientation. This ruled out the possibly that the charged plates are interacting with the earth’s electric field in terms of Coulomb forces. The second set of experiments conducted by Buehler was on parallel plate capacitors of equal physical dimensions with different separation distances, hence, altering the capacitance of the system. One such model was separated by a wax dielectric rather than air. Interestingly, polarity had no effect on the force on the plates, all of which moved away from the earth's surface. Although the capacitor with wax dielectric experienced dielectric breakdown rather early i.e. 31kV, it should be noted that until this point the change in mass experienced by the capacitor greatly outweighed the air dielectric versions. In addition, it should be noted that the capacitor with wax dielectric was fully enveloped in wax to avoid any ionization of surrounding air.

Buehler makes the important observation that the change in weight experienced by the capacitor plates is directly proportional to the amount of electrical energy stored in the electric field of the capacitor such that

$$force_{repulsion} \propto energy_{capacitor} \tag{8}$$

This means that the ability for the dielectric to store charge is directly proportional to the observed thrust. Hence, factors such as dielectric strength, plate size, and applied electric field are characteristic factors. Essentially the capacitance of the system is directly proportional to the thrust. An additional investigation is conducted by Buehler to observe the effects of accelerating charged particles from two oppositely charged wire grids such as those used by De Seversky [15] shown in Figure 12.Results on the experiments conclude that the electric grid movement was dependent upon orientation and polarity. This alludes to the fact that the force will always be in the direction of the emitter electrode which is consistent with other ionic wind experiments as discussed in section 2.1.2.

Further, Buehler makes a comparative investigation between ion wind and electrostatic forces with the earth's electric field. The experiment involved testing the performance of the ion grid and the charged plates in a faraday cage. Knowing that the force due to ion wind will still operate in the cage and that Coulomb forces require an external electric field and should not, insight into the thrust cause may be reached.

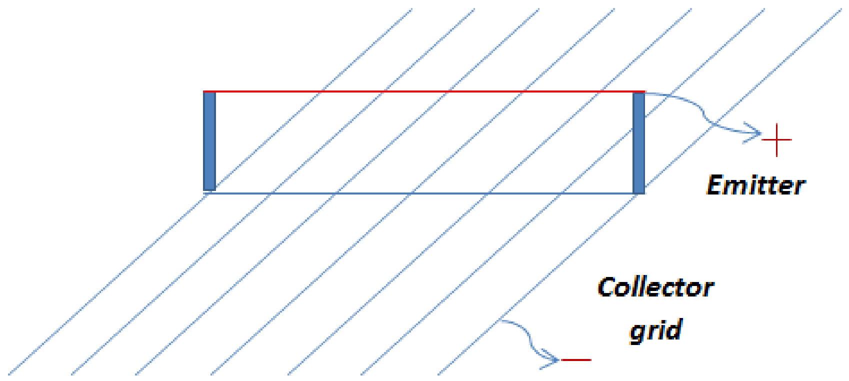

Figure 12 Ion Grid Setup used by Buehler

The results of the experiment followed these parameters i.e. the ion grid still experienced forces whereas the capacitor plates showed no sign of change in mass. This proves that the force on the capacitor plates cannot be attributed to ion wind and must rely on an external electric field. However, they still cannot be attributed to Coulomb forces with the earth's electric field because outside of a faraday cage the force is always directed away from the earth despite electrode polarity. Accordingly, Coulomb theory suggests that interaction with the earth's electric field would yield a force which changes with polarity changes. No explanation is provided by Buehler. Another experiment to gain further insight was performed with a circular parallel plate capacitor with air dielectric. To avoid the influence of the curved lines on the edges of the capacitor and the possible effects of an asymmetrical electric field, a guard ring was employed as shown in Figure 13. Weight reduction measurements were taken only from the centre capacitor where it was shown that the reduction in weight was identical to that without the guard ring. Hence, the influence of the asymmetrical field is not responsible for the thrust observed on the capacitor. Buehler concludes from his experimental investigation that high voltages consistently reduce the weight of single and parallel plate capacitors. No possible explanation is provided, although, Buehler rules out ion wind as the observed force, also Coulomb repulsion from the earth's electric field is also ruled out, albeit, the force is dependent on an external electric field. Essentially, Buehler claims that current electromagnetic laws cannot account for the movement on charged plates.

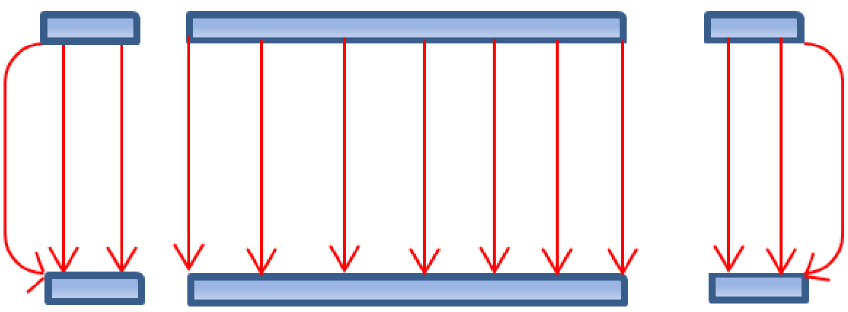

Figure 13 Symmetrical Capacitor with guard ring

Following the work of Buehler and the experimental conclusions that the effect is dependent on the earth’s electric field, a comparative study on measured self-potential variations of the Biefeld-Brown effect with the earth’s electric circuit is conducted by Stephenson in 2005 [27]. Fascinating parallels have been expressed between the observed weight loss of charged plates and activity of the earth’s electric field. Experimental measurements exhibit variations diurnal in nature as well as dependent on thunderstorm activity. Stephenson makes note of the peaks in the earth’s electric field due to thunderstorm activity matching the peaks of thrust measurements on charged plates. It is well known in atmospheric electro-hydrodynamics that the ambient electric field strength increases due to thunderstorm activity [30].

Although it was shown theoretically that it is not directly related to the earth’s electric field, some relationship obviously exists. Stephenson concludes that the anomalous force on charged plates is more an electrostatic rather than the electro-gravatic model as previously proposed by Brown[8].Hence, propulsion potential must be limited to earth’s electric field i.e. up to the earth’s surface to ionosphere.

2.2 EFFECT THEORY

2.2.1 Electro-hydrodynamics (EHD)

The thrust formed on highly charged electrodes of asymmetric physical dimensions belongs to the domain of electro-hydrodynamics. This particular phenomenon utilises basic physical principals such as Coulombs Law of Electrostatics, Newtons Third Law and the conservation of momentum principal to describe the force on an asymmetrical capacitor. The principal setup of the EHD thruster (or lifters) involves two electrodes whose radius of curvatures are of unequal physical dimensions such that $r_{c_{collecter}} \gg r_{c_{emitter}}$. A high voltage is supplied to the emitter each of the electrodes (whose particular orientation is not a defining factor) which results in the ionization of the surrounding fluid medium[31]. The collector electrode may remain either grounded or of opposite polarity. Since the radius of curvature of the emitter electrode is significantly smaller than the collector electrode, the electric field density is greatly asymmetric between the two. Once the corona is formed around the smaller electrode, an almost immediate attraction is formed between the collector electrode and oppositely charged ions. These ions are electrostatically attracted towards the collector electrode with which they collide and are discharged. The charged ion lands itself on the collector electrode which in turn generates the required current leak across the two electrodes [32]. In the process of travelling across the inter electrode gap these charged ions come into collision with neutral air molecules in the order or approximately 10^7 collisions per second[21]. The momentum imparted on the neutral air molecules by the charged ion projectile results in a downward wind known as ionic wind effect. The law of conservation would imply that the projected ion and neutral air molecule after colliding would travel in an equal and opposite directions. However, the ion is still under the influence of the electric field between the two electrodes and continues to travel along the electric field lines towards the collector electrode. After the collision with the charged ion, the neutral air particle continues its path downwards past the collector electrode and becomes what is known as the electric wind emanating from the EHD thruster. As a result of Newtons Third Law, the system experiences a reduction in weight equal to and opposite to the flow of wind.

2.2.2 Non-ionic wind theories

Several alternative theories surround the Biefeld-Brown effect although they have not been conventionally accepted by mainstream science due to the lack of knowledge in the field. One such proposal and the main proponent of electro-gravity is by TakaakiMusha[6, 33, 34] who explains the Biefeld-Brown effect as the result of an artificial gravitational field generated by the high potential electric field inside the atom. Musha observes the weight reduction of charged plates utilising alternating electric fields in experiments and believes this is caused by an interaction between the zero point field and the quantum vacuum of the charged field. Musha rejects ion wind as an explanation to the thrust by setting experiments in insulation oil to prevent effects of corona.

Only few proposed theories exist surrounding the effect which range from ether interaction theory[35] to unified field theories[36]that may hold the answers, however, they are yet to be fully incorporated into mainstream science.

Chapter 3 FLUID DIELECTRIC EXPERIMENTS

This chapter outlines and discusses a series of experiments aimed at understanding and providing scope for further enhancing thrust levels and efficiency. These experiments are conducted in accordance with electro-hydrodynamics (EHD) theory which requires extremely asymmetric electrodes immersed in a fluid dielectric medium.

3.1 INTRODUCTION

It was concluded from the literature that two schools of thought have formed since the discoveries made by Brown on the anomalous force between charged electrodes. The following chapter outlines the investigation into one such theory which surrounds the Biefeld-Brown effect, namely, the ionic wind theory governed by electro-hydrodynamics (EHD).This investigation is achieved firstly through an analysis of EHD theory followed by experimentally verifying that the force exists in a proof of concept experiment. Following, is a set of experiments which provide further insight into EHD theory and its mechanisms. Results obtained from the experiments are compared against those obtained throughout literature as well as the theoretical model for ion wind provided (section 3.2).

The experimental program is broken into two sections:

1. The first half of the experimental program involves a set of characteristic experiments which involve understanding the effects of geometry on the model. It is understood that ionic wind devices require an asymmetry between the electrodes such that one may act as the emitter (ionizing electrode) and the other the collector (grounded electrode).

2. Following from these characterization experiments a set of performance enhancing experiments are conducted which involve the use of magnetic fields and cross examination of the collector electrode radius of curvature in conjunction with electrode separation for enhanced thrust and efficiency.

3.2 THEORETICAL MODEL

3.2.1 Thrust

In order to find the expression for the force acting on the fluid medium (i.e. air) surrounding asymmetrical electrodes, the following assumptions are made[14, 17, 24]:

1. The electrodes are long relative to the gap length and the electrode radii ($L \gg d$, with L the length of the electrode)
2. The electric field in the gap is uniform and one dimensional
3. The emitter is at a potential V,
4. The collector electrode is grounded, $V_{Collector} = 0$,
5. The current is low enough that space charge effects do not significantly disturb the current output or electric field.

A uniform electric field is given by,

$$E = \frac{V}{d} \tag{9}$$

Collisions of ions appear as a drag force which acts opposite the electrostatic force, charge is transported at an average drift velocity, given by,

$$v_d = \mu E \tag{10}$$

Where μ is the ion mobility and E is the electric field strength. Defining current density using this drift velocity equation and defining a characteristic area A describing the area perpendicular to x occupied by ions,

$$j = \rho v_d = \rho \mu E \tag{11}$$

$$I = \int_S j \cdot dA = \rho \mu E A \tag{12}$$

Solving for charge density,

$$\rho = \frac{I}{\mu E A} = \frac{Id}{\mu V A} \tag{13}$$

Finally, solving for the coulomb electrostatic force on the volume of ions occupying the gap at any instant in time,

$$F = \int_V \rho E dV = \int \rho E A dx = \int \frac{Id}{\mu V A}\frac{V}{d} A dx = \frac{Id}{\mu} \qquad (14)$$

The use of this steady-state drift velocity in the above steps requires that the electrostatic force on the ions equals the drag force created by ion-neutral collisions. This drag force is equal and opposite to the drag force on the neutral fluid, which itself is equal and opposite the thrust felt by the thruster. Thus, electro-hydrodynamic thrust is expressed as,

$$F = \frac{Id}{\mu} \qquad (15)$$

In the case of this research the power supply is voltage controlled. Therefore, a particular voltage is set and current is drawn accordingly. The total current consumed by the corona discharge is approximated by,

$$I = CV(V - V_o) \qquad (16)$$

Where C is a constant depending on the electrode geometry[37]and ion mobility μ and V_o is the onset voltage at which a corona discharge forms and current flows across the electrodes.

The total power consumed by the discharge therefore becomes,

$$P = V \times I = CV^2(V - V_o) \qquad (17)$$

Substituting this into the thrust equation gives,

$$F = \frac{CV(V - V_o)d}{\mu} \qquad (18)$$

Hence, we are now left with the EHD force in terms of both voltage and current.

3.2.2 Effectiveness

The model to describe the effectiveness of the thruster and the one used in this research was formulated by Christenson and Moller [17]and used herein to describe the efficiency of the thruster at any given level of thrust. Hence the effectiveness is expressed,

$$\theta = \frac{F_{EHD}}{P} \qquad (19)$$

By inserting equations (7) and (9) we get,

$$\theta = \frac{Id}{\mu} \times \frac{1}{VI} = \frac{d}{\mu V} \tag{20}$$

This expression highlights that the effectiveness increases with $d$and decreases with ion mobility μ.

3.2.3 Wind velocity

Malik et al[38] describes the net thrust on the EHD model as a trade-off between electrostatic forces and the drag force of the collector electrode such that,

$$F_{EHD} = F_E - F_D \tag{21}$$

Hence, the drag force generated on an object moving through a fully encapsulating fluid medium is used,

$$F_D = \frac{1}{2} C_x . \rho . S . v^2 \tag{22}$$

Inputting equations (14) and (21) into (20) we get,

$$F_{EHD} = F_E - F_D = \frac{Id}{\mu} - \frac{1}{2} C_x . \rho . S . v^2 \tag{23}$$

Finally, solving for neutral air flow velocity, we are left with,

$$v = \sqrt{\frac{2(\frac{Id}{\mu} - F)}{C_x.\rho.S}} \qquad (24)$$

$\rho = 1.29\ kg.m^{-3}$is air mass density, S is surface area of collector electrode perpendicular to flow, *v*is neutral air velocity and $C_x$is the drag coefficient which we can safely assume for the geometry as $C_x = 1$[38].

3.2.4 Electromechanical efficiency

We derive an expression for the flow efficiencyη as a relationship between the neutral flow of air and the total force in terms of power drawn by the system such that [39],

$$\eta = \frac{P_{MECH}}{VI} \qquad (25)$$

Such that,

$$P_{MECH} = F \cdot u_{EHD} \qquad (26)$$

Where P_{MECH} is the mechanical power output, F is the generated thrust and u_{EHD} is the ionic wind velocity (ms^{-1}).

3.3 EXPERIMENTAL SETUP

The asymmetrical electrode model tested in this studyis essentially the same setup utilized by Brown in his 1960 patent[10] and what is now known conventionally as a ‘lifter’. The model utilises extreme asymmetry of the electrodes with the aim of generating a corona discharge around the smaller emitter electrode. Generally, ‘lifter’ designs vary in shape and size; however, in this study it consists of a lightweight insulating frame made from balsa wood to separate the electrodes.

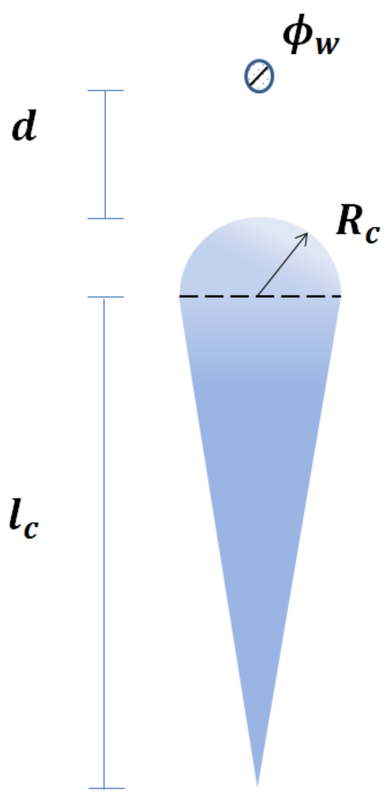

Figure 14 Cross-section wire-to-aerofoil design used in experiments

The basic components consist of an emitter electrode from copper wire and a larger collector electrode made from aluminium foil with a thickness$\delta = 0.25mm$, both separated by a specific allocated distance. This design is essentially a wire-to-aerofoil design whereby the aerofoil has an interchangeable radius of curvature and depth as shown in Figure 14. Traditionally, 'lifter' models consist of three cells[3, 40] in a triangular shape or more for other shapes and are made to lift off the ground. In this case of this research, however, a single cell is tested.

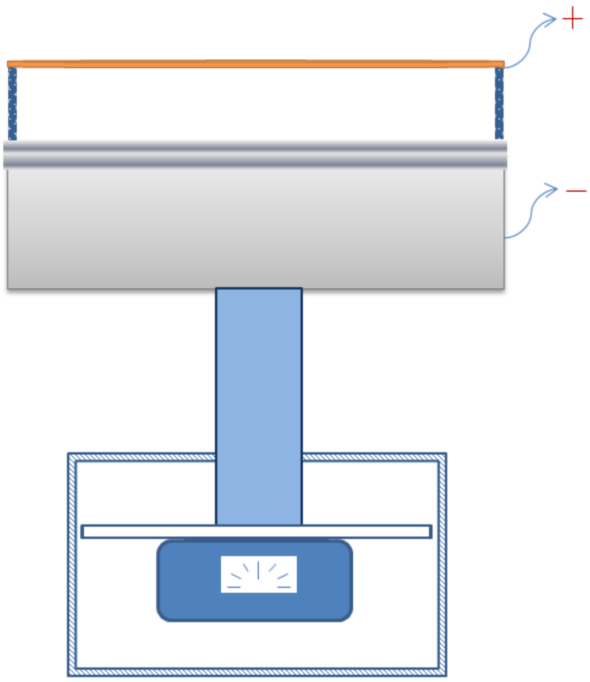

Figure 15 Experimental setup of following experimental program

The first set of experiments involves testing the characteristic variables which constitute the physical model. These include the wire diameter ranging from$\emptyset_w = 0.1mm - 1.25mm$, electrode separation distance from $d = 20mm - 160mm$, aero foil radius of curvature from $r_c = 5mm - 32.5mm$and aero foil depth from$l_c = 40mm - 60mm$. In addition, experiments are conducted which aim to characterize and understand the force and direction of wind emanating from the electrodes for further enhancement. It is through these experiments that insight is provided into the EHD mechanism and a second set of experiments are conducted which introduce magnetic fields and cross examining the variables against each other for enhanced thrust and effectiveness. This novel characteristic was founded through a deeper understanding of the electric field characteristics.

The model is set upon an electronic balance which is used to measure the change in mass at a precision level of±0.01g. In the setup up shown in Figure 15, the model lifter is set at a significant distance from the electronic balance and separated by an insulating material. This is done for two reasons; firstly, so any wind emanating from the model doesn't affect the scale reading due to its sensitivity and secondly, to allow a free path for the air to travel before it collides with any surface and in particular the scale. In addition, the electronic balance was placed within a faraday cage to eliminate any electromagnetic disturbances to the electronic balance due to projected ions.

Thrust measurements were taken as the change in weight from the original mass and the power to the craft was supplied via incremental steps in voltage. Hence, the voltage was increased every 2kV and maintained for a brief period of time. Power is delivered with to the electrodes with 0.11mm wire to avoid any obstruction load. From this point, measurements were taken from both the ammeter and the electronic balance. In literature, several studies have investigated the effects of changes in relative humidity[14] and EHD performance. In particular, Moreau et al [41] noted that RH below 50% results in an unstable discharge. Although, it was concluded that RH changes between 48-62% constitute minimal impact with a total effectiveness measurement error of approximately $\theta = \pm 1\, mNW^{-1}$. All experiments conducted in this research remain at a room temperature of 20˚C and a relative humidity maintained at 60%. The temperature and humidity were maintained in controlled environment facility to ensure consistency of results.

All units of current and thrust are expressed span-wise such that current is expressed as $\mu A\ m^{-1}$ and thrust mNm^{-1}. This does not affect the total reading as it has been shown that current is proportional to the length of the model such that,[40]

$$\frac{I_M(V)}{L_M} = \frac{I_N(V)}{L_N} \tag{27}$$

Where I_M and L_M are the input current and total length of thruster M and I_N and L_N are the input current and total length of thruster N and V is the voltage at any time.

3.4 CHARACTERIZATION EXPERIMENTS

3.4.1 Proof of concept

The first experiment conducted aims to act first and foremost as a proof of concept to the theory of ion-wind. To this end, an EHD model is built, tested and compared with theoretical data concerning EHD theory to provide validation to this particular explanation.It should be noted that all experiments will be conducted with a positive corona. It has been found that positive coronas are the superior mechanism for enhanced thrust and efficiency[18, 23].This is partly explained by the fact that the mobility of negative ions is higher than that of positive ions. In addition, Moreau et al [41]show in their experimental results that differences between positive and negative are minimal over gaps of 30mm where the mobility of ions tends to become equal.

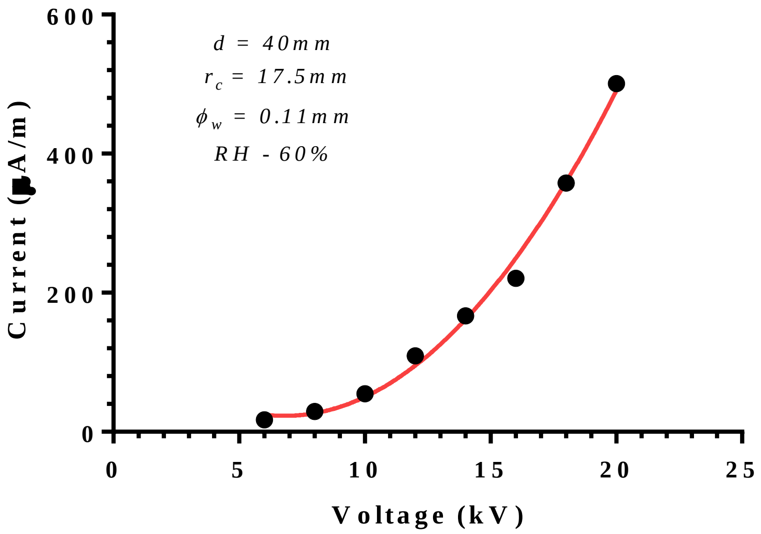

Figure 16 Current versus Voltage (I-V)

The EHD model tested consists of an emitter electrode diameter$\emptyset_w = 0.1mm$, an inter electrode gap $d = 40mm$ and a collector electrode diameter and depth of $r_c = 17.5mm$ and $l_c = 40mm$ respectively resulting in a thickness-to-chord ratio of 0.6.

We can see from the I-V graph in Figure 16 the current measured against voltage (I-V). The curve shown is fitted from equation 16 and shows that the measurements match well with the theoretical expression from which we interpolate a value for the constant C which is $C = 1.81\mu A\ \mathrm{k}V^{-2}m^{-1}$. This compares well with values obtained by Moreau et al [41]where C was in the order of $2.27\mu A\mathrm{k}V^{-2}m^{-1}$ for wire-to-cylinder configurations at a gap of $d = 30mm$. In addition we derive an onset voltage value of $V_0 = 5.466kV$ for the 40mm electrode separation which is also consistent with literature [3, 40, 41].

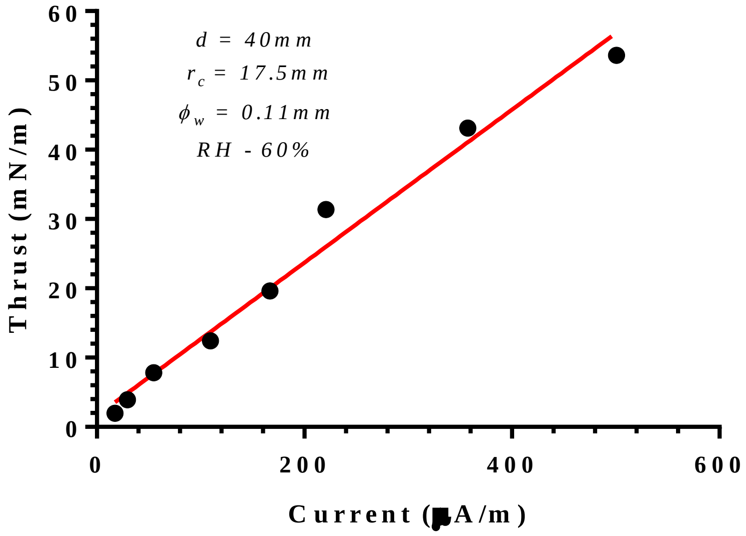

a

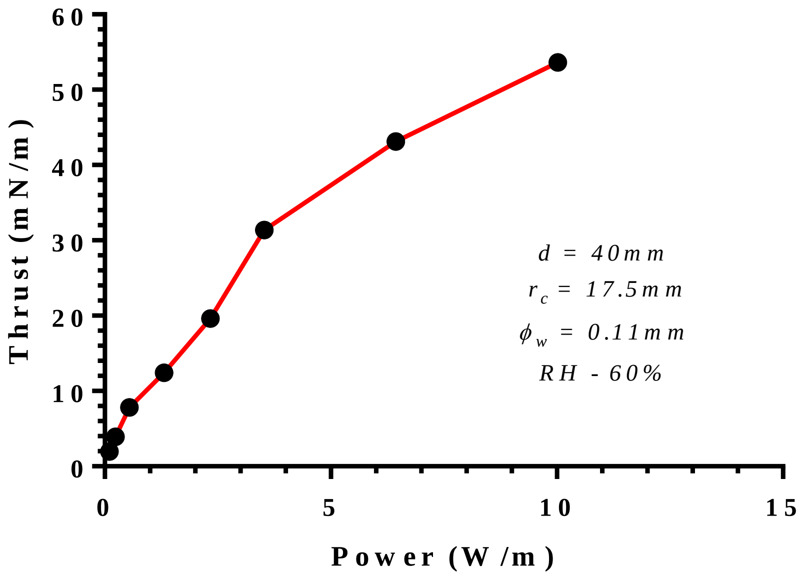

b

Figure 17 (a)Thrust versus current (T-I), (b) Thrust versus Power (T-P)

Figure 17 (a) and (b) show the thrust per unit length (mNm^{-1}) with respect to current (T-I) and thrust versus power (T-P) respectively. From Figure 17 (a) we see that thrust is directly proportional to the discharge current across the electrodes as expressed in equation15 such that $F \propto I$ resulting in a curve equal to $115.4NA^{-1}$. By interpolating with experimental data we may determine the ion mobilityμ across the discharge region. We see that the mobility in this case for a positive corona is $\mu^{+} = 2.636 \times 10^{-4}m^{2}V^{-1}s^{-1}$.This is in agreement with literature where ion mobility usually ranges from $\mu^{+} = 1.8 - 3.5 \times 10^{-4}m^{2}V^{-1}s^{-1}$[39, 41]depending on the electric field and surrounding dielectric medium.

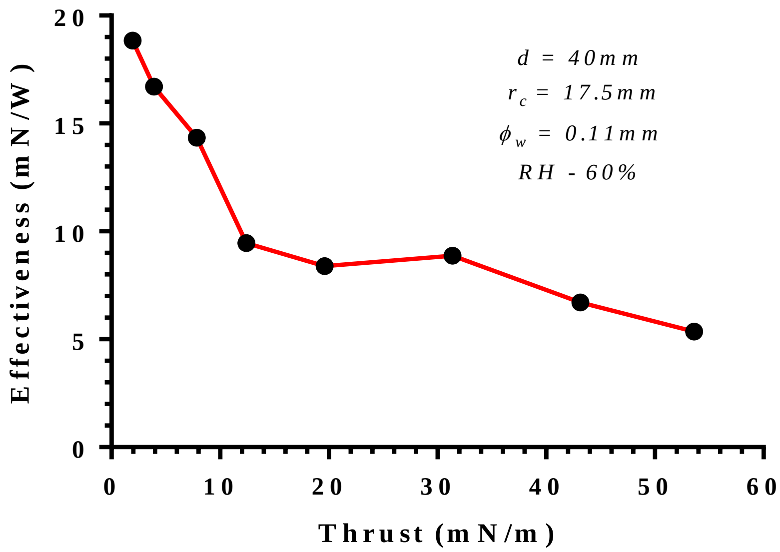

Figure 18 Effectiveness versus Thrust (θ-T)

Thrust vs power (T-P) shown in Figure 17(b) illustrates how the maximum thrust diminishes as extra power is injected into the corona discharge. We observe from this data that there exists an asymptotic ceiling on the thrust performance as power input increases. This highlights that power input is the governing parameter of thrust performance.

Figure 18 illustrates the effectiveness versus thrust plot (θ-T) such that as the thrust of the experimental model increases the effectiveness of diminishes. This is consistent with results previously found in literature [23, 41]. Additionally, this result correlates well to the theoretical formulation of Pekker and Young [14] which expresses that the thrust diminishes with increased power input as shown in equations 5 and 6 whereby the EHD thruster system will always have a receding efficiency with thrust. We notice in this particular case that the optimum effectiveness is$\theta = 18.84mNW^{-1}$ at$1.96mNm^{-1}$ of thrust.

In fulfillment of one of the thesis objectives we have constructed and experimented with model wire-to-aerofoil models in a fluid dielectric medium. Results have been compared and analysed with respect to other experimental research as well as the theoretical model for EHD thrust in section 3.2. It has been shown that the observed thrust and thrust performance on asymmetrical electrodes are in accordance with an electrostatic model governed by EHD principals. We may conclude from the proof of concept case that the discoveries of Brown which describe a force between extremely asymmetric charged electrodes immersed in air are in fact the result of ionic-wind. The remainder of the chapter now aims to characterize the fundamental geometry of the model wire-to-aero foil thruster for a more in-depth understanding of EHD phenomena and performance enhancement.

3.4.2 *Wire Diameter*

The aim of this experiment is to examine a variety of wire diameters in order to test their impact on thrust and efficiency. A previous study into the characteristics of emitter electrode geometry for increased efficiency and thrust levels which was conducted by Wilson for NASA in 2009[23]. Wilson experimented with a multitude of different emitters including wire, pins and razor blades with various spacing's. These tests aimed to demonstrate the feasibility of increasing thrust and flow velocity using more complex geometries-in reference to needle to plate etc. Wilson concluded that pin emitters performed better than wires as they required a lower inception voltage V_o. It was also deduced from the experiments that spacing between pins of 29mm was the optimum separation distance. In addition, smaller tip radius showed the greatest overall performance, however the smallest tips with initial radius of 2μm displayed effects of erosion after several tests. Another in-depth analysis by Moreau et al[41] found that the although pins did result in lower discharge current requirements, the thrust to current conversions were in favour of wire electrodes due to the higher ion mobility generated from the pin electrodes. Moreau et al also found that the thrust to effectiveness levels between the two were relatively similar. Hence, Moreau et al concluded that the difference between wire diameter and needle tip is not of real concern, but rather, the radius of curvature of the emitter electrode was of importance, which should be as small as possible. Therefore, in order to wholly understand the impact of the emitter electrode diameter for the wire-to-aerofoil models used in this thesis, four different sized copper wires are selected and tested. The four wires have diameters $\emptyset_1 = 0.1mm, \emptyset_2 = 0.5mm, \emptyset_3 = 1mm, \emptyset_4 = 1.25mm,$ respectively.

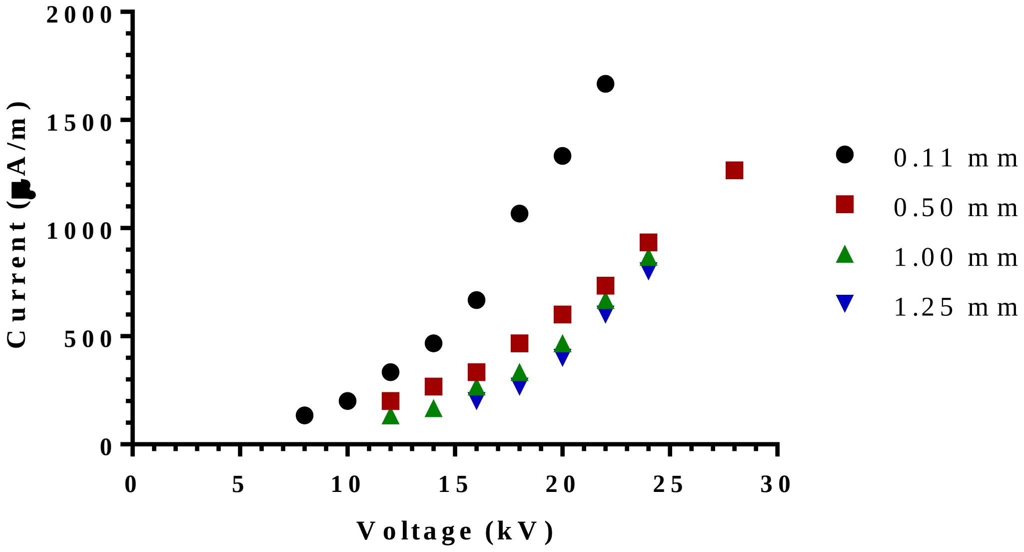

Figure 19 Current vs voltage (I-V) for emitter electrode diameters

Figures 19, 20 and 21 represent the I-V, T-I and T-P graphs respectively. Immediately we observe that the smaller emitter electrodes induce higher current levels for a given voltage input. This may be attributed to the generation of corona at lower inception voltages as shown in Table 1. From the T-I plot in Figure 20 we see clearly that as the wire diameter increased the thrust produced decreased with respect to current and from the T-P plot in Figure 21 we observe that the thrust versus power values of larger wire diameters are relatively low. All results point to the benefits of a smaller wire diameter for optimal thrust to input power levels.

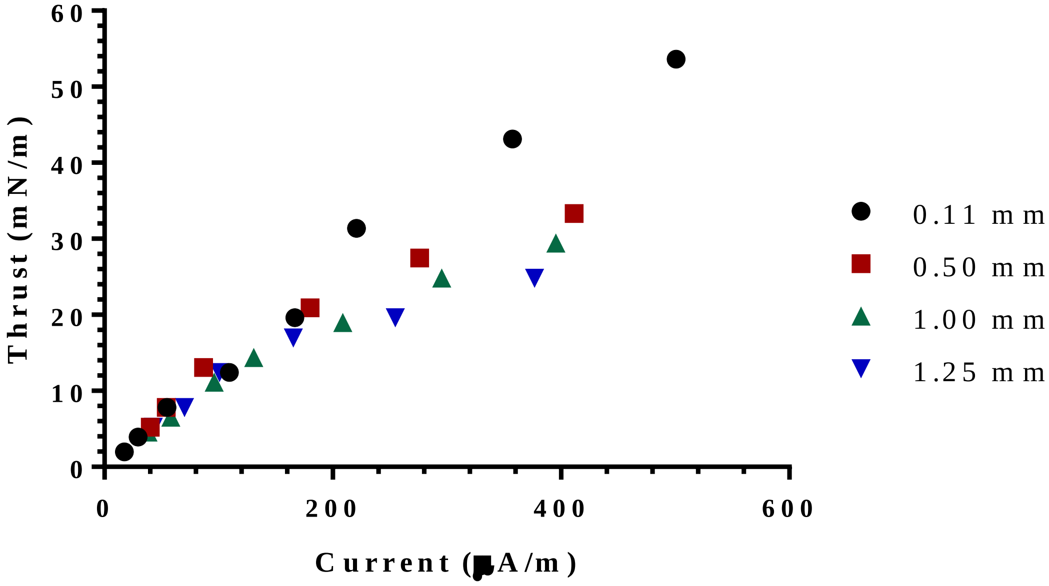

Figure 20 Thrust vs current (T-I) for emitter electrode diameters

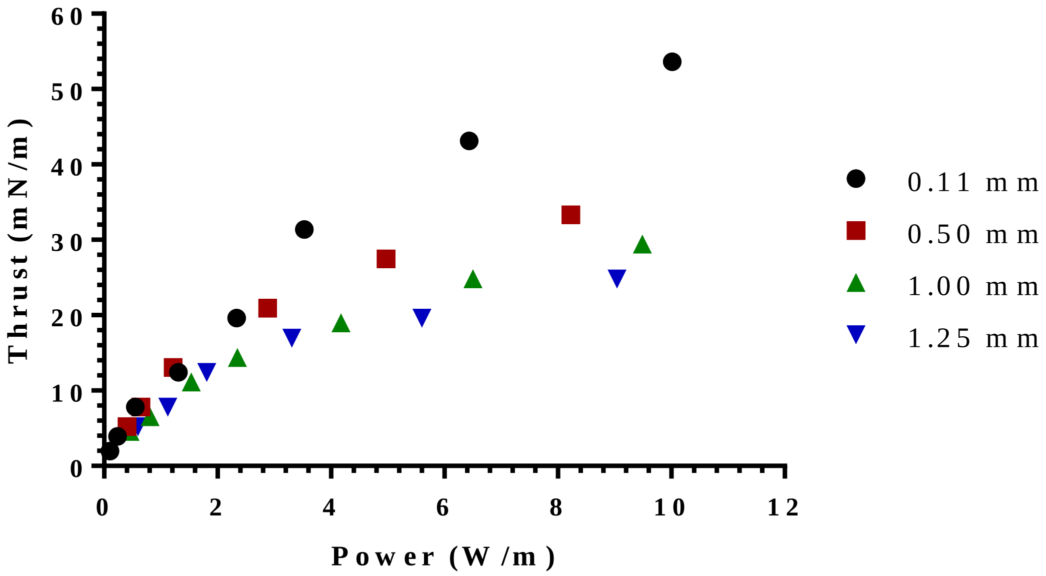

Figure 21 Thrust vs Power (T-P) for emitter electrode diameters

Table 1 outlines the mobility of ions μ^+, the constant C and the inception voltage V_o of the different emitter electrode diameters. Interpolating with equation 15 we see why the thrust levels per current input decrease with emitter electrode diameter - the mobility of ions increases from $3.47 - 5.24 \times 10^{-4} \mathrm{m^2 V^{-1} s^{-1}}$ between the 0.11mm and 1.25mm wires. We also see that the corona inception voltage increases with the wire diameter which is also found in literature [40]. This alludes to the fact that enlarged diameters require a higher voltage for a corona discharge to form between the electrodes.

Table 1 Values of μ^+, C and V_0 for different emitter electrode diameters

Wire Diameter (mm)	**μ^+ ($10^{-4} m^2 V^{-1} s^{-1}$)**	**C($\mu A kV^{-2} m^{-1}$)**	**V_o(kV)**
0.11	3.47	1.81	6.961
0.5	4.36	1.615	8.297
1	4.82	1.0427	9.304
1.25	5.24	0.9907	10.163

Finally, we observe from the θ-T plot in Figure 22 that the maximum efficiency levels are obtained from smaller emitter electrode diameters. It is understood that the sole purpose of the emitter electrode is to generate a corona discharge in the normal glow region with as little power input as possible.

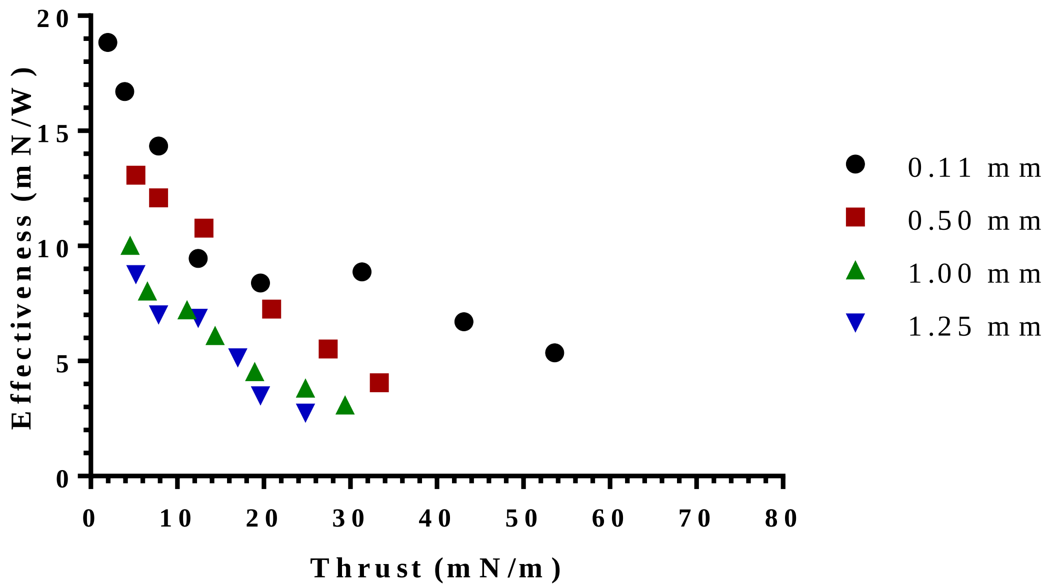

Figure 22 Effectiveness vs thrust (θ-T) for emitter electrode diameters

Therefore, it may be concluded from this experiment that the ability for the emitter electrode to effectively generate a corona discharge around itself, is a function of its radius of curvature; a variable which is optimum at smaller diameters.

3.4.3 Electrode Separation

The aim of this experiment is to understand the effect of inter-electrode distance on the observed thrust and efficiency of the EHD thruster. Experimental research conducted by Wilson[23] finds that the optimum separation between electrodes on pin-to-plate configurations exists at 57 and 70mm with tests spanning 19-95mm. However, despite lower current measurements at equal voltage, larger gaps were seen to display increased values for θ. In addition, Moreau et al[41] also conclude as part of their characterization on wire-to-cylinder work that larger separation gaps do indeed produce more effective thrust on experiments ranging from 10-40mm. As a result their model improved by approximately 5.5N kW^{-1} to 17 N kW^{-1}between 10mm and 40 mm separation. The EHD model used in this experiment is identical to the one used in the previous experiments which utilises an emitter electrode diameter of $\emptyset_w = 0.1mm$and collector electrode radius of curvature $r_c = 17.5mm$, relative humidity and temperature are maintained at 60% and 20˚C respectively. A series of gaps is examined ranging between 20mm and 160mm.

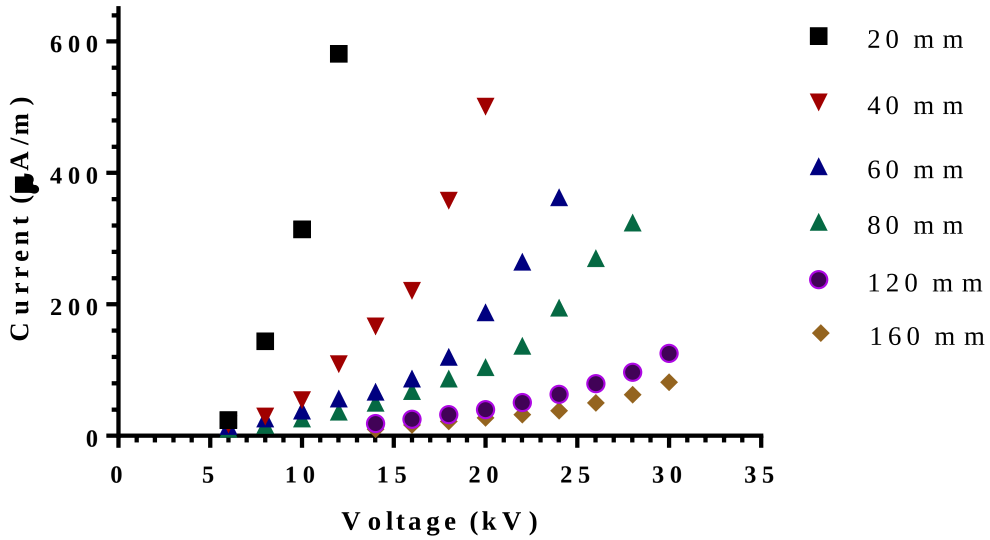

Figure 23 Current versus Voltage (I-V)

Figure 23 outlines the I-V data points for the selected inter-electrode gaps. As was expected, as the gap increases the discharge current decreases with voltage. Essentially, one may conclude that smaller gaps require less power. This means that smaller amounts of power are utilised by smaller separation distances to generate the same current flow across the electrodes.

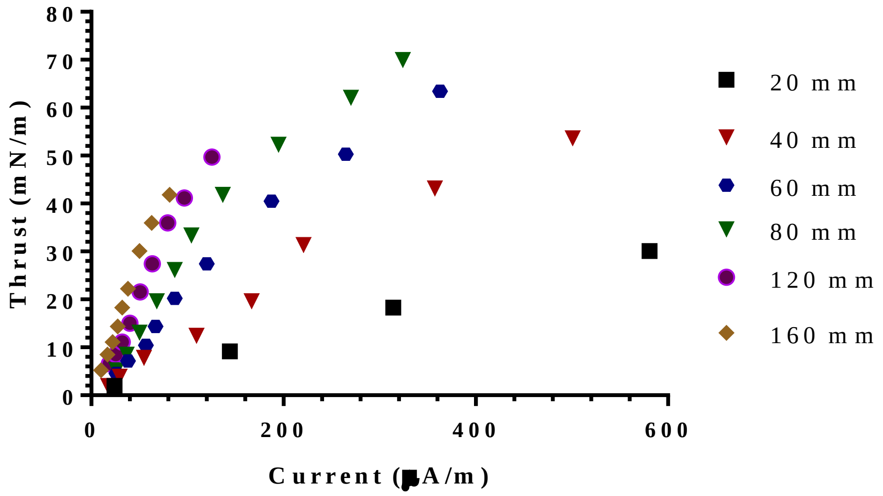

a

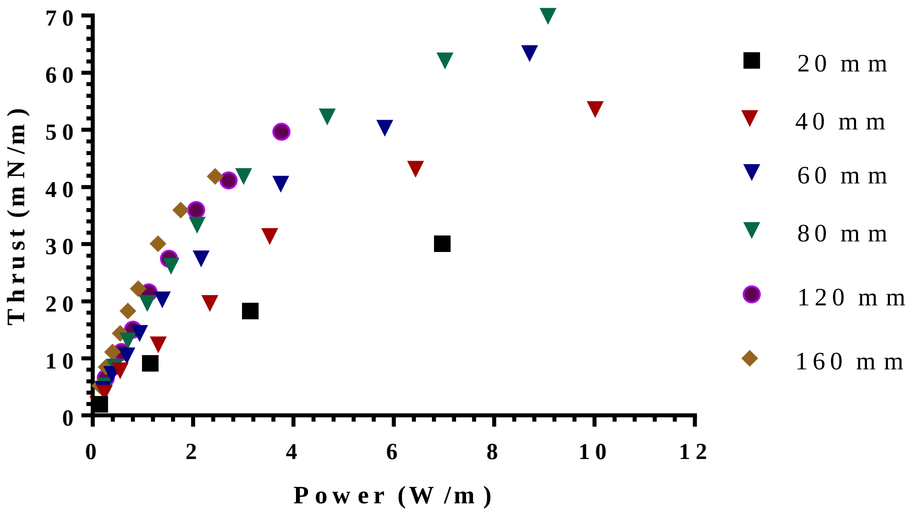

b

Figure 24 (a) Thrust versus Current (T-I), (b) Thrust versus Power (T-P)

Studying the T-I graph in Figure 24 (a) we see that the data points may be correctly interpolated into equation 15, once again indicating that the thrust is directly proportional to input current. In addition, we see that the increase in thrust should essentially be proportional to electrode gap. Hence, we see in the Table 2 that the ion mobilityμ^+ remains relatively constant, verifying the theoretical data.

Table 2 also outlines the interpolated value for the constant C and the onset voltageV_o. We see that as the inter electrode gap increases,V_o increases while C decreases. This may be explained by the fact that as the gap is increased the voltage input required to generate a current discharge increases to facilitate the additional distance. It is also demonstrated through equation 18 that the value of C is proportional to inter-electrode gap such that $C \propto \frac{1}{d}$.

Table 2 Values of μ^+, C and V_0 for different electrode separation gaps

Electrode Separation (*mm*)	**μ^+ $(10^{-4} m^2 V^{-1} s^{-1})$**	**C$(\mu A kV^{-2} m^{-1})$**	**$V_o(kV)$**
20	3.72	7.483	5.614
40	3.47	1.81	6.961
60	3.16	0.83	7.557

80	3.3	0.537	7.922
120	2.9	0.183	8.554
160	2.91	0.119	8.770

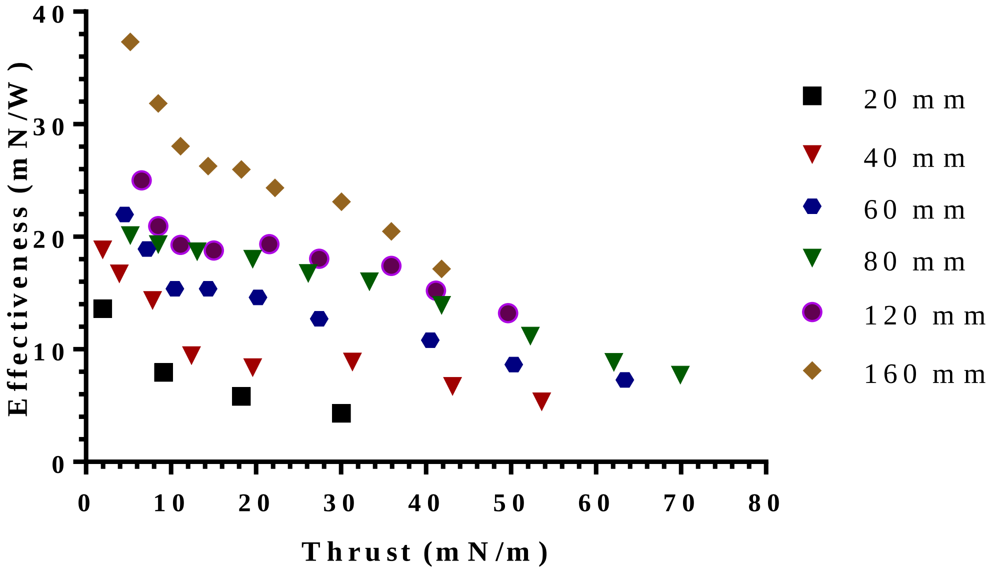

Figure 25 Effectiveness versus Thrust (θ-T) for different electrode gaps

Looking at the θ-T plot in Figure 25 we see an almost direct relationship between the separation gap distance and effectiveness to thrust ratio. Comparing these results to Moreau et al [41] we notice an almost identical resemblance at $d = 40mm$. It is quite clear that increasing the electrode gap is a very effective method of ascertaining more efficient thrust. This observation is in accordance with equation 20 where $\theta \propto$

d.Literature claims that obtaining $\theta \geq 20NkW^{-1}$[17, 23, 41] is required to make EHD thrusters valid for propulsion purposes; this study achieved $37.3NkW^{-1}$ at $5.23mNm^{-1}$ of thrust. This immediately indicates that EHD thrusters have potential for propulsion purposes when utilising large electrode separations.

3.4.4 Aerofoil Depth

The aim of this experiment is to observe the effects of increased foil depth on thrust performance and efficiency. It is a well-known characteristic of electrostatics that the electric field lines emanating from the small electrode tend to expand and position themselves across a larger surface area of a larger electrode. This concept is illustrated in Figure 26 where the electric field lines from the tube wrap around the circular electrode.

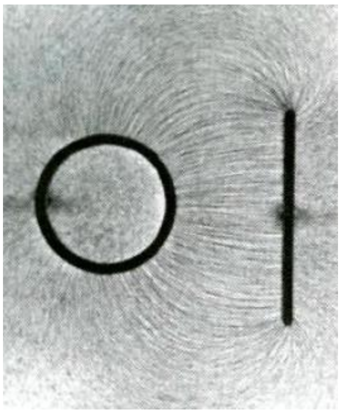

Figure 26 Electric field lines as a result of asymmetric electrodes [42]

This concept may be applied to EHD thrusters whereby it is assumed that the asymmetrical electrical field lines travel far down the collector electrode. By varying the aerofoil depth it may be possible to utilise a greater amount of the electric field i.e. projected ions.

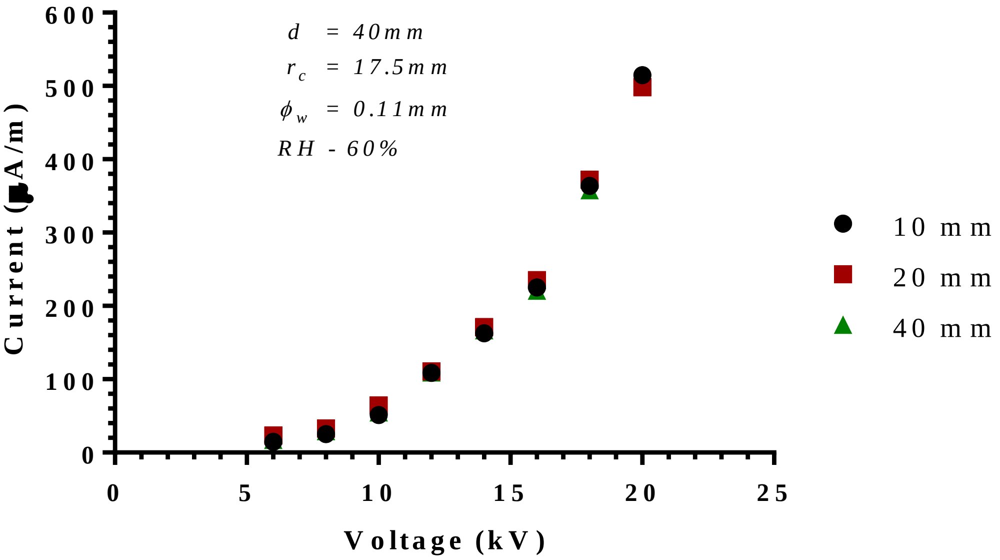

Figure 27 Current versus Voltage (I-V) of different aerofoil depths

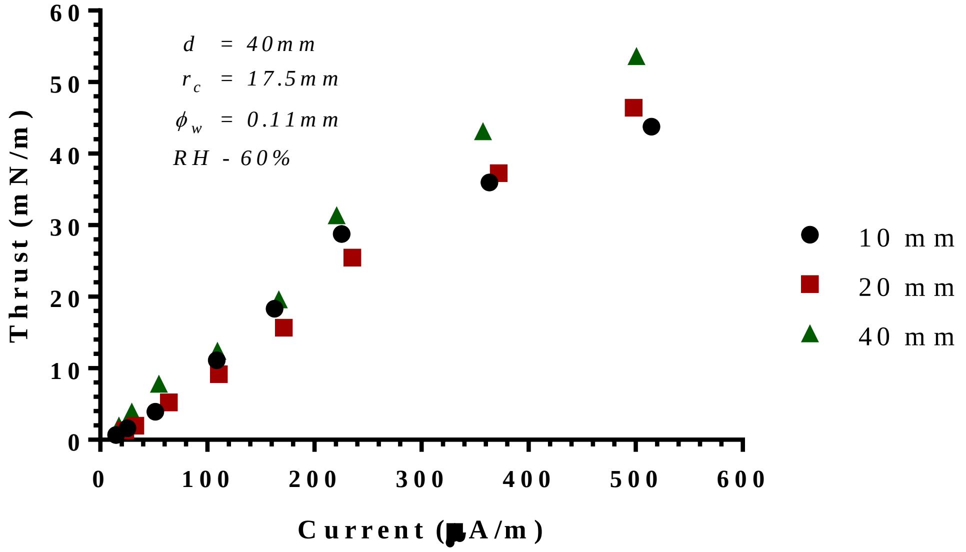

Figure 28 Thrust versus Current (T-I) for different aerofoil depths

The three foils depths were tested on the wire-to-aerofoil model were $l_c =$ $10mm, 20mm$ and$40mm$. The wire diameter was left at $\emptyset_w = 0.1mm$ and the separation between electrodes and radius of curvature of the aerofoil remained $d = 40mm$ and $r_c = 17.5mm$ respectively.

Figure 27 outlines the I-V plot for different aerofoil depths. It is obvious that there is a negligible effect by the foil depth on the I-V relationship. It may be concluded that the enlarged aerofoil depths do not change the discharge qualities of the model thruster. Figures 28 and 29 outline the T-I and T-P curves respectively, it can be seen that as aerofoil depth increases the level of thrust increases with corona discharge current and power. From these results we may conclude that enhanced thrust with larger aerofoil depths is attributed to the fact that as the area of the collector electrode increases, more electric field lines are encountered which assists in the total electrostatic force between the aerofoil and positive ions in the corona discharge region. Chung and Li [40] also obtain similar results with their collector electrode depth experiments yielding slightly better thrust to power results as electrode depths increased.

Figure 30 displays the θ–T plot; we see that the 40mm foil depth results in the greatest effectiveness especially at lower thrust levels. The observations of this asymmetry are consistent with an electrostatic explanation for the effect despite the relatively minimal impact. Table 3 outlines the constant C and onset voltage values for the different aerofoil depths. The constant C remains relatively similar across the depths indicating that the change in depth is of minimal concern and does not affect the impacting geometry.

This may be explained through the work of Kiousis et al [39] who models the corona current distribution in space using multi-physics modelling software to show that the normalized current density distribution on a wire-to-cylinder EHD setup. Electric field flow lines outline the path of ion trajectories which terminate at a specific angle θ. It is concluded that the contribution of current density beyond 80^{o} has minimal effect.

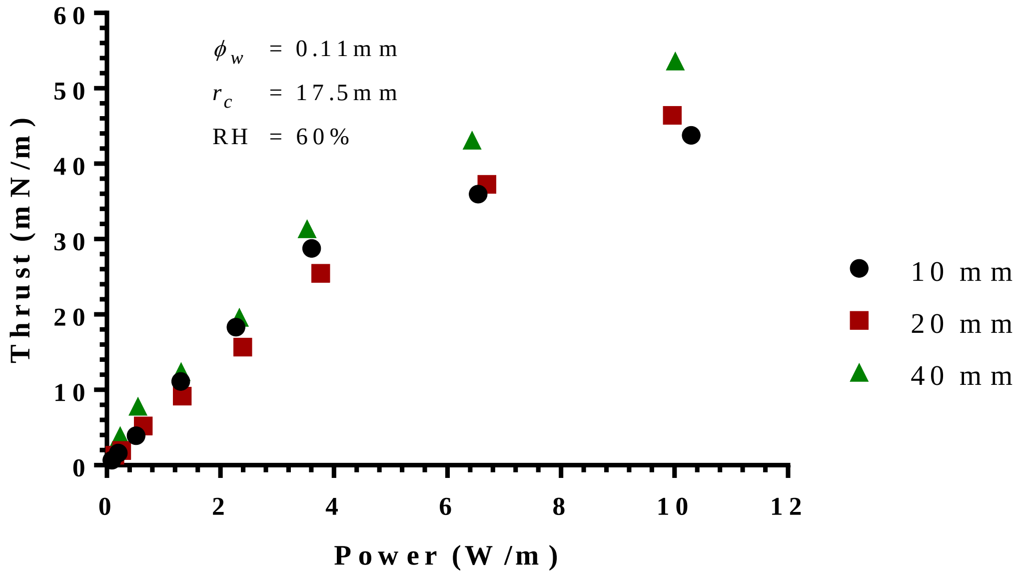

Figure 29 Thrust versus Power (T-P) for different aerofoil depths

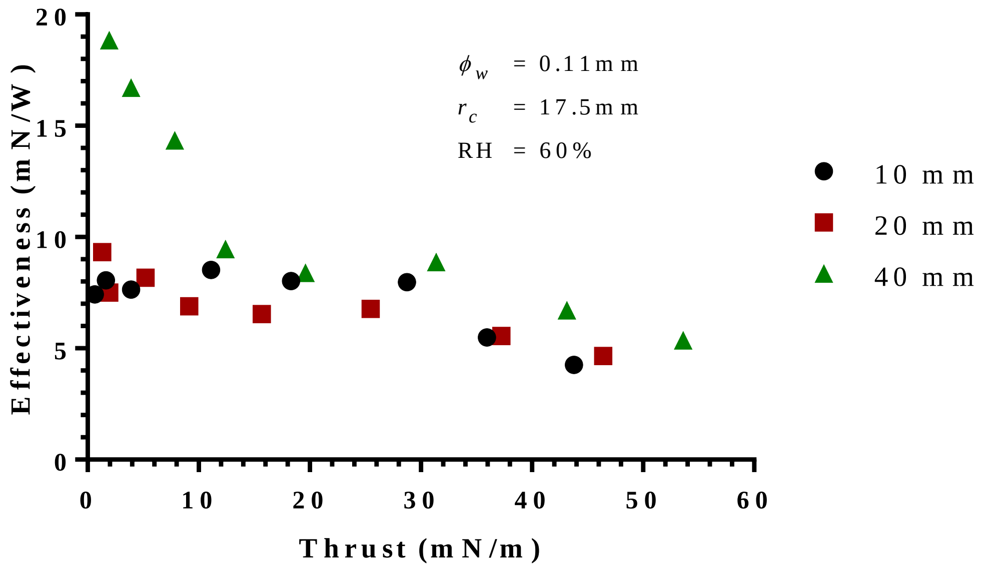

Figure 30 Effectiveness versus Thrust (θ -T) for different aerofoil depths

Hence, a correlation may be drawn between the increase in aerofoil depth and slight increase in thrust and effectiveness. Essentially, the increased depth may come into contact with more electric field lines interacting at lower values of θ, although this diminishes with distance.

Table 3 Values of C^+ and V_0 for different aerofoil depths

Foil Depth (mm)	C^+ ($\mu AkV^{-2}m^{-1}$)	V_0 (kV)
10	1.9069	5.614
20	1.7679	6.496
40	1.81	6.961

3.4.5 Radius of curvature

The aim of this next experiment is to observe how the collector electrode radius of curvature affects the generation of thrust on the wire to aerofoil configuration. The creation of wind from the EHD thruster is a direct result of the extreme electrode asymmetry which aids in the corona discharge properties. The ability for the collector electrode to draw the oppositely charged ions provides one the primary constituents to the function of the ion wind device. Therefore, we now explore an experiment which aims to examine the effect of this asymmetry between the electrodes through varying the aerofoil radius of curvature. Additionally, preliminary tests with the simple EHD models indicated that thrust depended greatly on the presence of a radius of curvature of the collector electrode. In addition, it was shown in the experiments of Canning et al[22] and Bahder and Fazi[9] that the asymmetrical capacitor thrusters which utilised a collector electrode radius of curvature performed exceedingly better. The inter electrode separation and emitter diameter are $d = 40mm$ and $\emptyset_w = 0.1mm$ respectively. Three different aerofoil radius of curvature models were constructed and tested consisting of $r_c = 0.5mm, 17.5mm$ and $32.5mm$. Aerofoil depth was maintained at $l_c = 40mm$. Figure 31 displays the I-V plot where it is seen that there is a slight increase in the current to voltage curves as the radius of curvature increases.

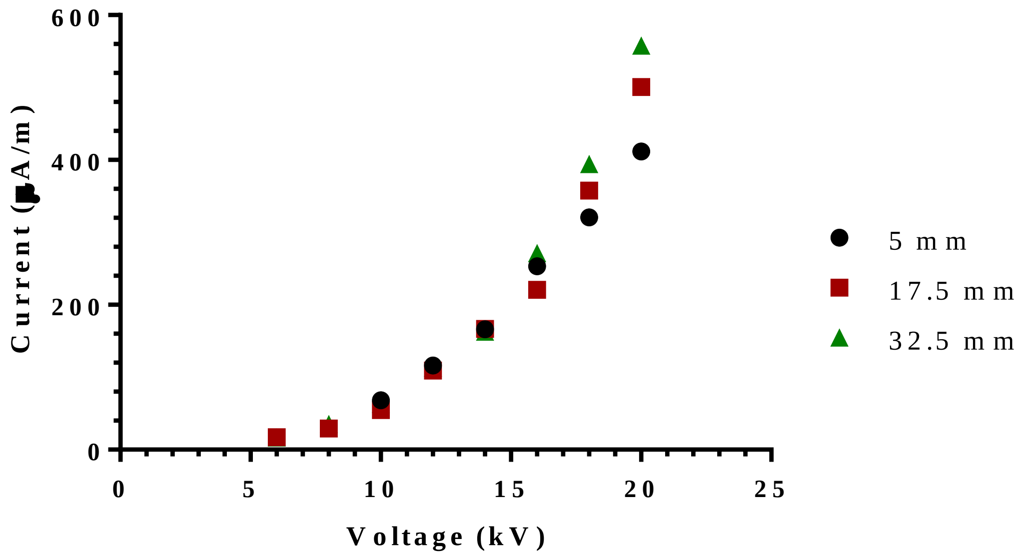

Figure 31 Current vs Voltage (I-V) for different collector electrode radii

Figure 32 displays the T-I plot where it is observed that at low currents the thrust levels are higher for larger diameters. However, as the current rises this changes so that the smaller radius of curvature produces more thrust. This observation also coincides with the θ-T plot in Figure 34. Here we observe that the larger collector radii are more effective at low thrust and small radii are more effective at larger thrust levels.

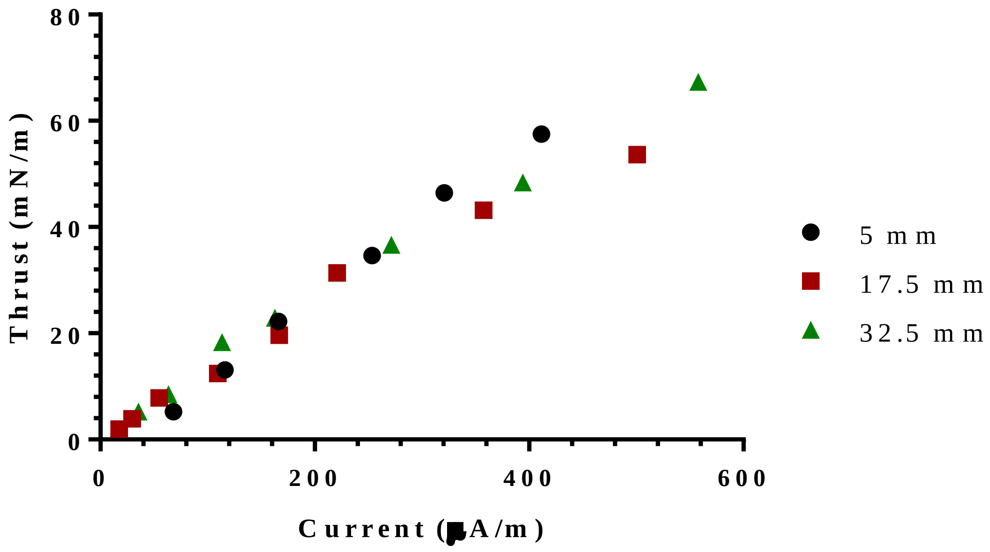

Figure 32 Thrust vs Current (T-I) for different collector electrode radii

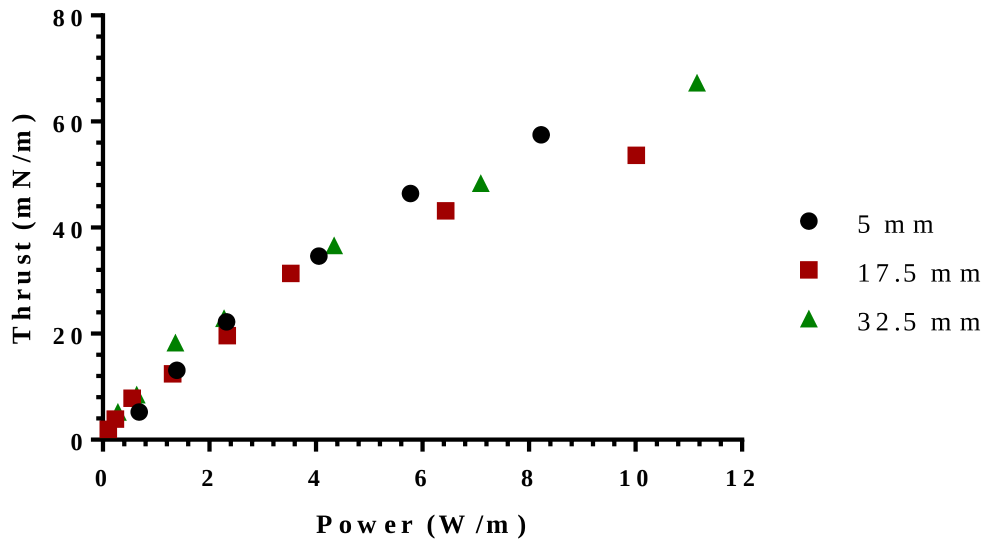

Figure 33 Thrust vs Power (T-P) for different collector electrode radii

This observation may be attributed to the low velocity of neutral air at low power inputs, hence the large electrostatic force is overpowering. Contrarily, as the wind velocity increases at larger currents the larger radius of curvatures would begin disrupt the neutral air flow. At lower power inputs the wind is negligible and therefore unaffected by the collector electrode size.

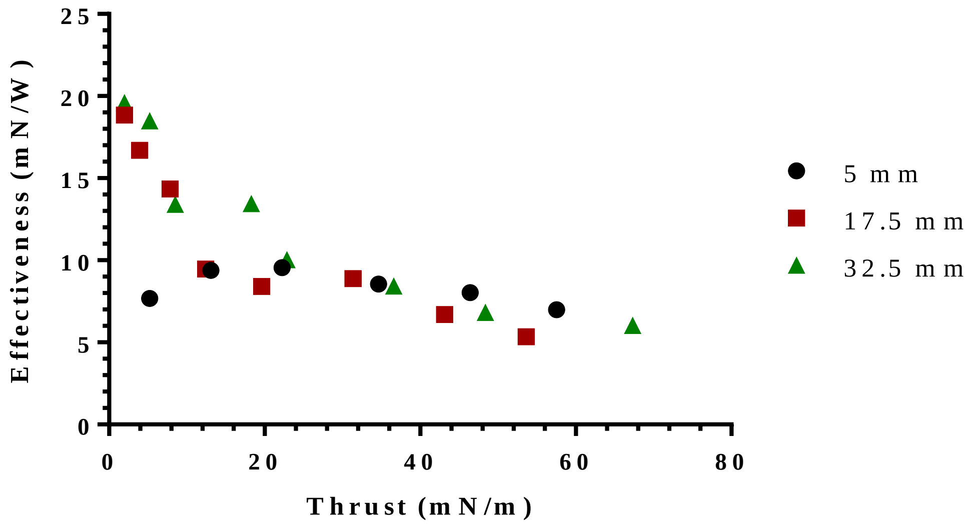

Figure 34 Effectiveness vs Thrust (θ-T) for collector electrode radii

We may conclude at this point, that at a separation of $d = 40mm$ the optimum collector electrode radius of curvature lies between 5mm and 17.5mm. However we may conclude, in accordance with Moreau et al[41] and Chung and Li[40], that the radius of curvature does not seem to impact performance levels with the same magnitude as electrode separation or emitter electrode diameter.

3.4.6 Air Flow Characteristics

The final characterization experiment conducted, aims to understand the magnitude and direction of wind around the charged electrodes. This is achieved through smoke and flame experiments which provide further insight into possible enhancement methods. In addition, it was expressed in the theoretical model for EHD thrusters that the total force on the system is a trade-off between the drag of the system and electrostatic forces as shown in equation 21. In the previous experiment which examined aerofoil radius of curvature, we observed that larger radii have a negative impact at larger currents due to its obstruction on neutral air flow. For this reason, the following wind velocity experiments are conducted on series of collector electrode geometries which constitute an equal surface area in order to determine the optimum thruster configuration. The inter electrode separation and emitter diameter are $d = 40mm$ and $\emptyset_w = 0.1mm$ respectively. The smoke and flame tests are conducted on the wire to aerofoil configuration with aerofoil depth $l_c = 40mm$ as in previous experiments.

Flame and smoke tests on the model indicate the direction of flow around the EHD thruster. It is obvious from Figure 35 (a) that once the flame stick was placed perpendicularly to the corona discharge region, the flame was pulled in between the electrodes. This is as expected as ions are projected from the emitter electrode downwards; surrounding air is constantly returning to fill the region. On the other hand, the flame placed near the surface of the collector electrode showed that the air moved in a direction towards the aerofoil and down its surface.

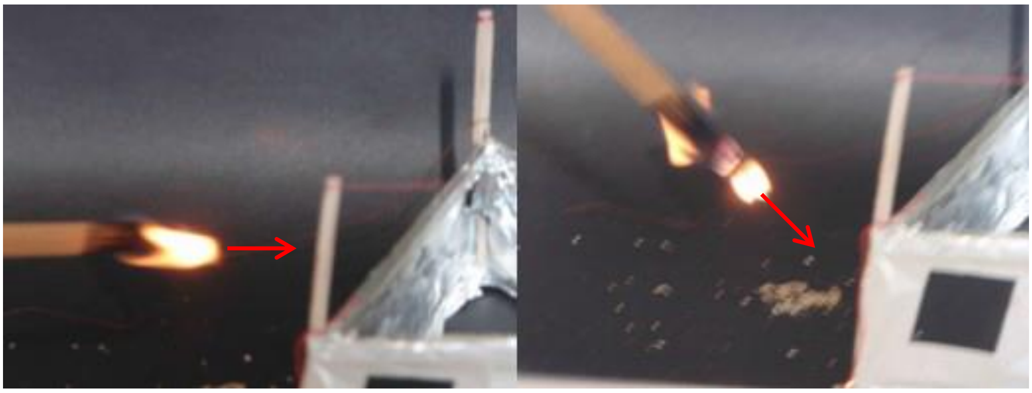

a

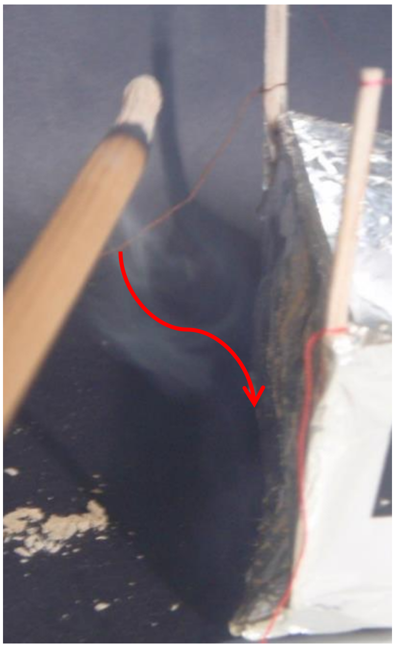

b

Figure 35 (a) Flame tests showing direction of surrounding air into corona discharge region, (b) Smoke test showing flow moving towards and down collector electrode

This is further confirmed with smoke tests. It can be seen that the direction of wind is clearly towards the larger electrode and downwards in the curved fashion as shown in Figure 35 (b).

Thus, it may be concluded that the flow of neutral air is towards the corona discharge and down the sides of the collector electrode. Consequently, an experiment is conducted which aims to alter the shape of the larger electrode to enhance the flow of wind for increased thruster performance. To this end, we characterize the ionic wind velocity profile for different collector electrode shapes which support the same collective surface area. Hence, a section of Aluminium sheet $150mm \times 150mm$ was moulded into different plane shapes for the collector electrode. Results were taken for the aerofoil geometry used in earlier experiments compared with collector electrode sides going straight down, horizontally, cylindrically, curved and bell arced as shown in Figure 36. It should be noted that although $r_c = 0.5mm$ will remain, the depth of the collector electrode will vary with each geometry.

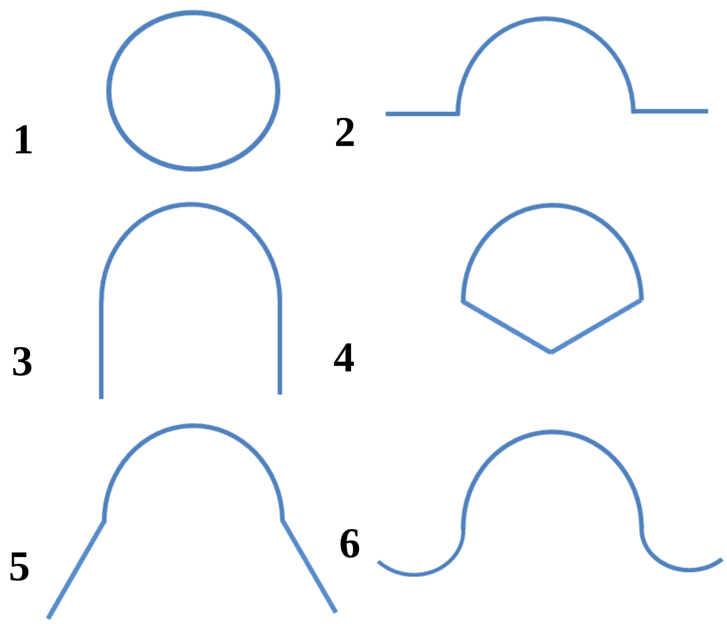

Figure 36 Different collector electrode geometries

Although, it would have been very insightful to characterize the flow of air around the collector electrode upstream, it was not possible to get readings in the inter-electrode gap due to the high voltages and corona discharge. Therefore, air flow measurements were taken across the horizontal axis of the EHD thruster 30mm below the trailing edge in order to characterize the airflow downstream. Points A, B, C and D in represent the wind velocity locations; point A indicates the centreline location and point C being slightly off the trailing edge of the aerofoil. The method of detecting the magnitude of wind around the lifter was the hotwire device with a ±3% precision rating. The hotwire is placed on a retort stand at the specified locations below the thruster. The results provided in Table 4 indicate the thrust obtained by the model thruster as well as the maximum magnitude of air flow of each shape at 20kV.

Table 4 Thrust and air velocity measurements

Collector Electrode Shape	**Thrust (g)**	**Maximum Air Velocity (m/s)**
4. Aerofoil	0.82	0.75
3. Straight Down	0.79	0.8
2. Horizontal	0.44	0.58
6. Double curve	0.4	0.22
1. Cylinder	0.7	0.65
5. Bell shape	0.61	1.12

We see from Table 4 that the bell shaped collector electrode displays the highest wind flow despite not producing the largest amount of thrust. This solidifies the trade-off between electrostatic and drag forces expressed in equation 21.Additionally, this also explains why some wire-to-plate configurations have diminished thrust levels; due to the blocking of the wind resulting in a negative thrust effect [41]. Please note that the numbers in Table 4 under 'collector electrode shape correspond to the numbers in Figure 36.

Figure 37 displays the velocity profiles of each shape at 20kV. It is evident from the reading obtained by the hotwire device that the magnitude of air velocity is strongest when moving downwards by the surface of the collector electrode with exception to the aerofoil and cylinder designs. Point C signifies the point slightly beyond the surface of the collector electrode.

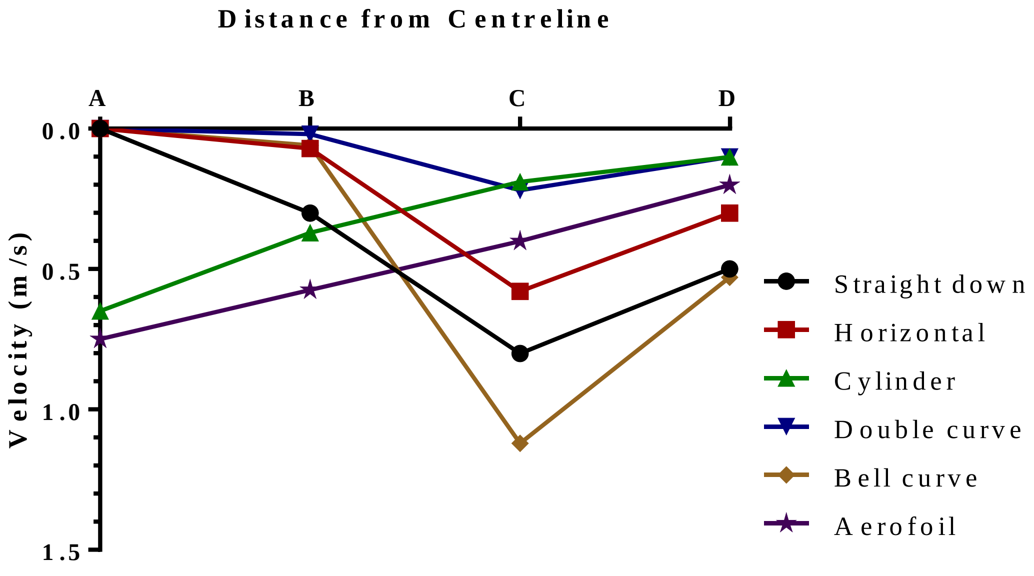

Figure 37 Wind velocity profile for different collector electrode geometries

The results may be compared with findings by Martins and Pinheiro for the Institute for Plasmas and Nuclear Fusion [43], show similar results in terms of the magnitude of air in certain positions. It can be seen from the numerical simulation that air velocity is greatest around the bottom electrode which directly parallels to the results obtained by the hotwire device. In addition, a research was conducted by Malik et al in 2014[38] which also aimed to determine the air flow velocity surrounding the larger electrode. They come up with a model based off the conventional electro-hydrodynamic model to describe ion drift which determines the expected velocity of wind caused by the thruster. Deriving from equation 24 at $16kV$ they ascertain a value of $0.7366m.s^{-1}$. These results were compared to experimental data which used particle image velocimetry (PIV) to obtain values in the range of $0.7 - 0.8\,ms^{-1}$. These values correspond very closely to the results obtained by the hotwire device in this research.

3.5 ION WIND EXPERIMENTS

3.5.1 Effect of Magnetic Field on Thrust Generation

The aim of this experiment is to understand the impact of an external magnetic field on the thrust performance of the EHD model. The magnetic field was created using a neodymium rare earth permanent magnet 20mm x 5mm x 12mm. The magnet has a rating of N35 which corresponds to a magnetic field strength between 1.17-1.21T. The EHD model used is essentially the same wire to aerofoil configuration used in previous experiments with an emitter electrode diameter and aerofoil radius of curvature of $\emptyset_w = 0.1mm$ and $r_c = 17.5mm$ respectively.

The neodymium bar magnet was placed slightly above and parallel to the wire with orientation shown in Figure 38 (position A). Results were taken initially for the reduction in weight of the single cell lifter with and without the influence of the magnet.

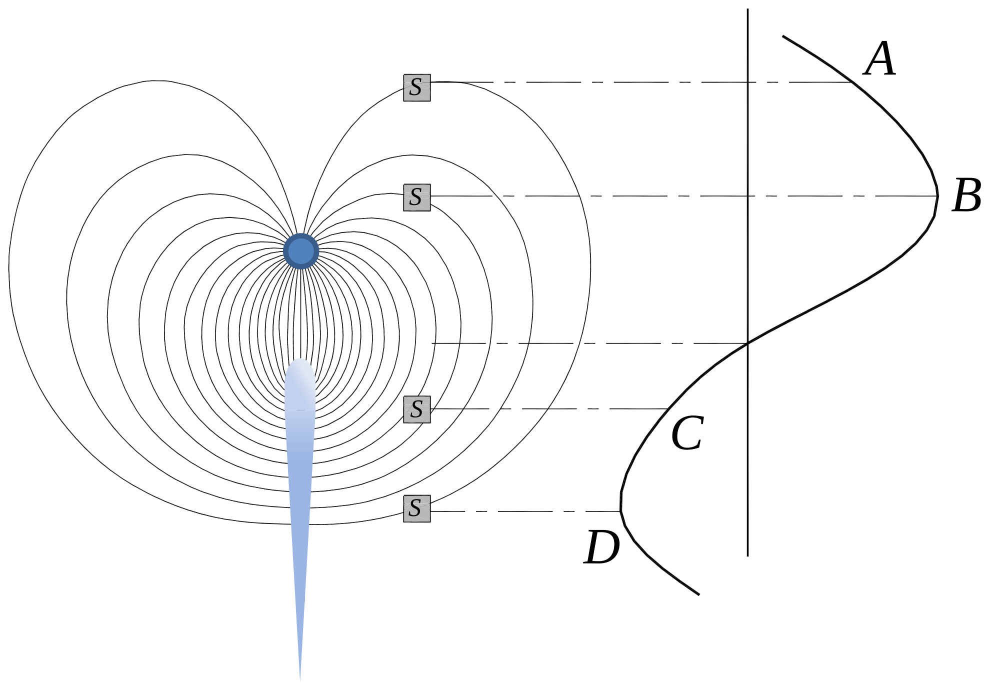

Figure 38 Cross sectional view of EHD model with various magnet locations

It can be seen from Figure 39 that there is a significant reduction in weight of the lifter with the influence of the permanent magnet. It can also be seen that the influence of the magnet increases as the voltage increases. This result correlates directly to the fact that as the electric field strength increases, the velocity of charged particles increases. The force on a charged particle in a magnetic field is directly proportional to this velocity as shown in Equation 26.It can thus be seen that a magnetic field influences the thrust observed on asymmetrical electrodes. These results support the ionic wind theory, it is shown that the Lorentz force applied to charged ions increases their downward momentum. It is now important however, to determine at which location this magnetic field is optimum.

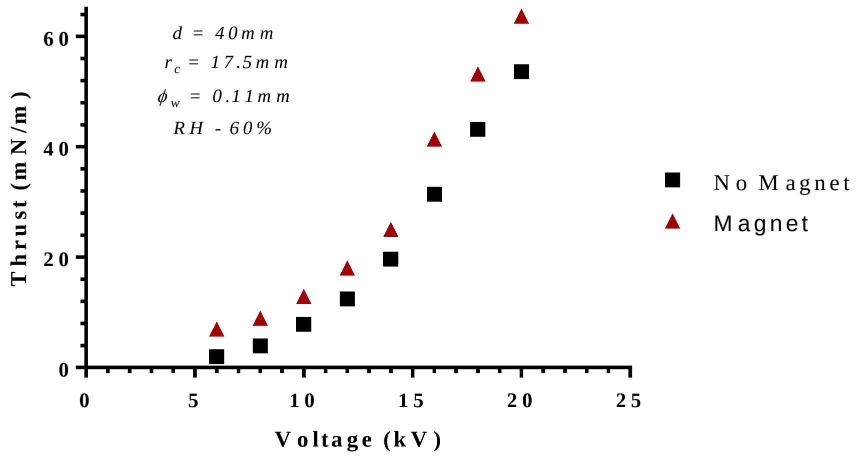

Figure 39 Thrust vs Voltage (T-V) with influence of magnetic field

It is well known that the force on a charged particle due to a magnetic field is expressed by the equation

$$F = qvBsin\theta \quad (27)$$

Where q is magnitude of charge on the particle, v is the velocity of the charged particle and B is the magnitude of the magnetic field. $Sin\ \theta$ represents the angle at which the magnetic field and direction of the motion of the charged particle interact. This means that the maximum force experienced by a charged particle is perpendicular to the magnetic field lines. As can be seen in Figure 38, a permanent magnet was placed at various locations around the asymmetrical electrodes. Due to the unequal dimensions of the electrodes, the electric field lines are as shown[9, 43]. This means that positively charged particles would travel along these lines towards the larger collector electrode.

Figure 41 outlines the angle of a positively charged ion as it enters the magnetic field of the permanent magnet. The result force between the two fields is also shown as determined by the 'right hand rule' [42]. As a result, the maximum thrust observed on the asymmetrical capacitor is when the permanent magnet is placed at point B. This is exhibited by the fact that the force is directed almost directly downwards. This would impart the greatest force on the particles moving in this direction. This is by virtue of the electric field lines; the trajectory of the positive ions crosses the magnetic field lines with a value of θ closest to 90° at this point.

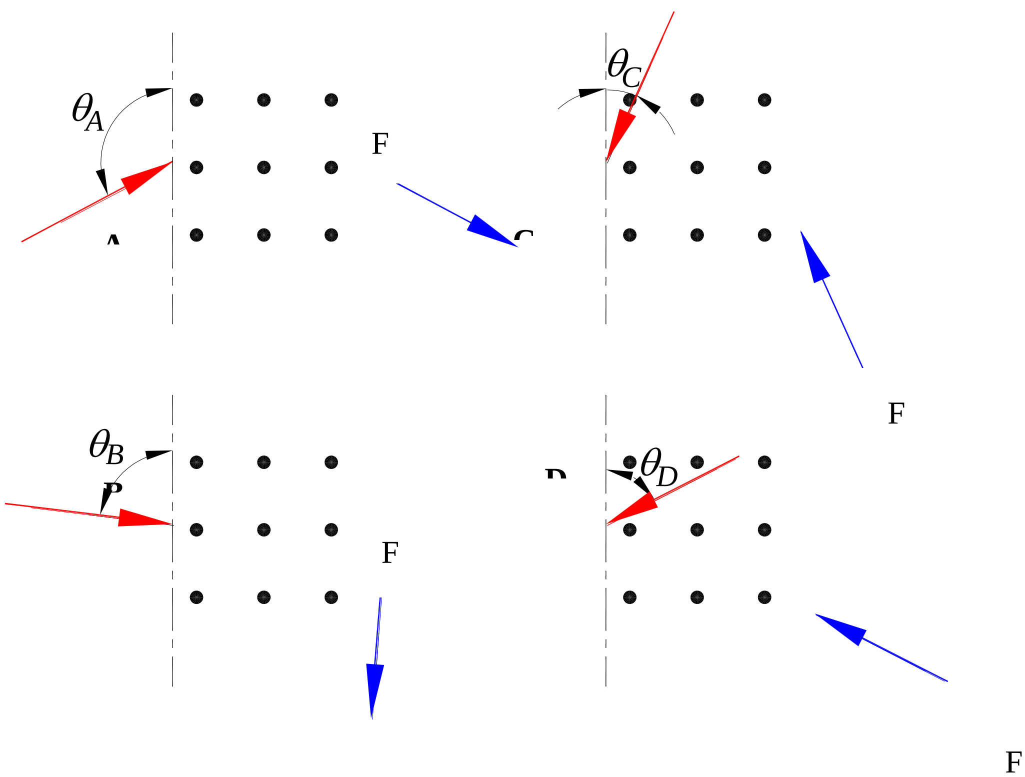

Figure 40Positively charged particles in magnetic field out of the page

Interpolation into equation 27 would result in a maximum value. It can be seen from the resultant force at D, that the magnetic field actually results in a negative effect on the positively charged particles pushing them in the upward direction. This decreases the velocity of the charged ions. A decreased velocity would result in a lower collision energy with neutral air particles and hence, less lift. This theoretical analysis of the ion trajectory in electric and magnetic fields correlates directly to the experimental results. The change in weight of the single cell lifter was measured with the permanent magnet placed in positions A, B, C and D. Thrust measurements were taken at both 17.5kV and 20kV as shown in Table 5.

Table 5Thrust measurements at various positions at 17.5kV and 20kV

	Weight of lifter (g)	
Magnet Location	**@17.5kV**	**@20kV**
No Magnet	38.3	53.6
A	45.4	61.2
B	47.4	63.6
C	44.1	59.7
D	41.6	56.5

Experimental data expressed in Table 5 shows that the EHD thruster experiences its greatest largest thrust when the permanent magnet is placed at position B. This observation is shown for an asymmetrical electrical field at two potential differences solidifying the results. It can therefore be concluded that charged ions emanating from the positive corona around the wire are accelerated by a magnetic field. This induced force is maximised when the charged ions enter the field at perpendicular angles. Not only do these results provide a new avenue for increasing thrust performance characteristics of the effect but it also provides further evidence that ion wind plays a role in the thrust observed on asymmetrical capacitors.

3.5.2 Independent Forces on Electrodes

A notion of extreme importance required to fully grasp an understanding of the force observed on asymmetrical electrodes involves determining the magnitude and direction of the thrust on each electrode individually. EHD theory suggests that ions emanating from the emitter electrode collide with neutral particles; as a result a flow of wind is generated resulting in upwards lift. It was even observed in the collector electrode shape experiment discussed earlier that obstruction to the neutral air flow had a negative impact on thrust measurements. However, the question arises as to whether the observed thrust is electrostatic of hydrodynamic in nature. Subsequently, an experiment is conducted which involved measuring the change in mass of the electrodes individually yet in order to come to stronger conclusions on the cause of thrust.

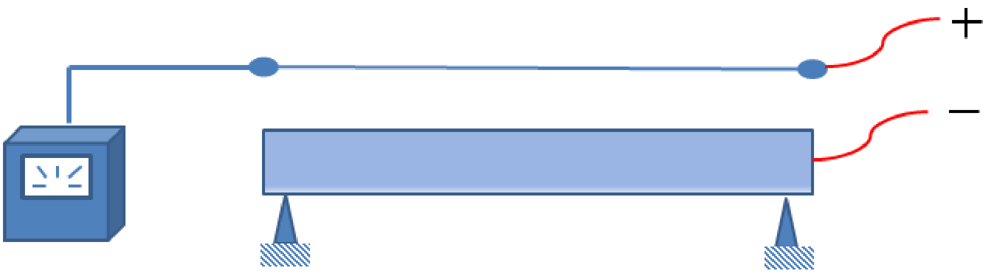

a

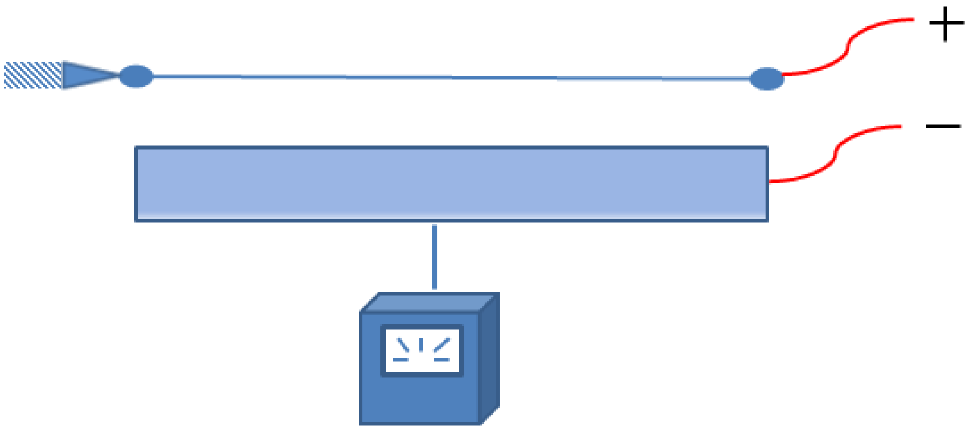

b

Figure 41 Experimental setups (a) emitter electrode (b) collector electrode

Figure 41presents the experimental setup whereby the change in mass of each electrode on the electronic balance is measured individually. The basic components of the experimental setup have remained as in previous experiments with $d = 40mm$, $\emptyset_w = 0.1mm$ and $r_c = 17.5mm$. Shown in Table 6, it was observed that the change in mass of the larger electrode was essentially the change in mass which is experienced by the system as a whole in previous experiments. There is an almost negligible change in mass in the smaller electrode in the magnitude of 0.01g which, in addition, was measured as an increase in mass.

Table 6 Independent electrodes thrust measurement

	Thrust (mN/m) @20kV
Whole Configuration	53.6
Small electrode	6.53
Large electrode	48.5

It is made evident by this experiment that the force observed by the asymmetrical electrodes is induced on the larger electrode. In addition, it is observed that there is actually an attractive force between the electrodes which is outweighed by the larger electrode. Two possible explanations are made which can explain this effect. The first explanation is that as air is pushed downwards across the large electrode, viscous forces across its surface result in a reactionary force which induces lift. This however, cannot be the case. It has been seen in several experiments in literature [13, 29]that the effect may be produced on mesh wires acting as the larger electrode. These wires do not have the capacity to generate lift through viscous forces. Therefore the second and more probable explanation is that there exits an electrostatic attraction between the large electrode and the ion cloud generated around the smaller electrode. As ions travel down towards the large electrode, the electrode is attracted upwards. In addition it is believed that the small electrode is attracted to the large electrode by an electrostatic force also, through the build-up of electrons on the surface of the larger electrode. The attractive forces between the electrodes is greatly outweighed due to the dense electric flux around the smaller electrode compared with the large electrode; a concept which was put forward by Canning et al to explain the movement of their asymmetrical capacitors [22].

Martins and Pinheiro[43] developed a numerical model to express the nature of the force on asymmetrical electrodes. It is deduced that the production of wind is a secondary effect and that it is purely electrostatic in nature; in excess of 97.7% of the total force. In this experiment the collector electrode measured 86.5% of the total thrust. In addition, it is concluded from the study that the large electrode will experience majority of the force due to charge separation which remains neutral in its total charge.

3.5.3 Cross Examination of Electrodes

Previous experimental investigations in section 3.4 into variables such as wind velocity, electrode separation and the independent forces experiment in section 3.5.2 have shown that the ability for the collector electrode to collect projected ions and manoeuvre neutral air flow greatly affects the constant C, $\mu^{+}$and the overall effectiveness of the EHD model. An abundance of experimental research into the emitter electrode exists whereby many researchers conclude that the observed thrust on EHD devices is limited to certain maximums as a result of increased input power[14, 16]. This was first expressed by Christenson and Moller[17] and further iterated by Pekker and Young[14] who believed ionic wind devices did not have a future as a propulsive device.

Additionally, Matsuyama and Barrett [24] makes note that an unexplained performance degradation was observed in a thruster model at larger values of current. This was noticed, despite equation 15 predicting a linear variation of thrust with current; above a certain threshold, gradient ${}^{dF}/_{dI}$ was seen to decrease into a second linear regime. Matsuyama hypothesises that, as applied voltage is increased, a second corona discharge of opposite polarity is ignited at the collector electrode. This however, is not believed to be the case because for collector electrode geometries which are far in excess of the CIV still suffer from the same performance hindrance.

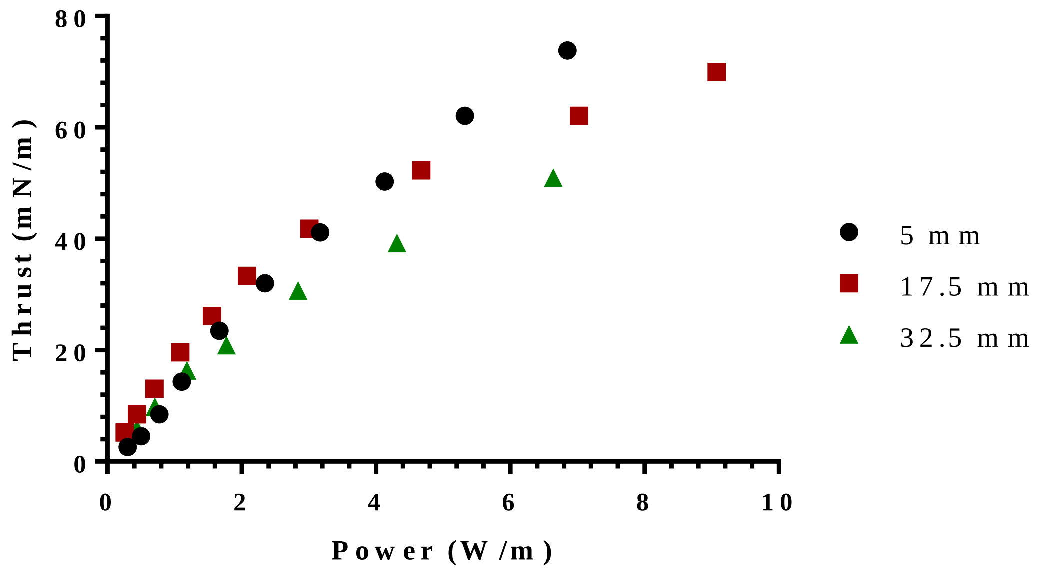

Figure 42 Thrust vs power (T-P) at 80mm separation

Unfortunately, little research has gone into enhancing the larger electrode. A characterization study conducted by Moreau et al[41] touched upon collector electrode diameter concluding that its impact did not play a key role. Wilson[23] also conducted an intense research on emitter electrode geometry with wires and pins. However, the only emphasis on characterising the collector electrode was an experiment which tested more than one electrode for a single emitter. Wilson found that optimum results were observed for two collector electrodes located approximately 30mm apart. Kiousis et al [39] also did an analysis of radius of curvature ranging 0.5mm -15mm concluding that the increasing discharge current, thrust and wind from increasing curvature. This however is not paralleled in this research where increased radius of curvatures up to $r_c = 32.5mm$ resulted with negative performance at $d = 40mm$

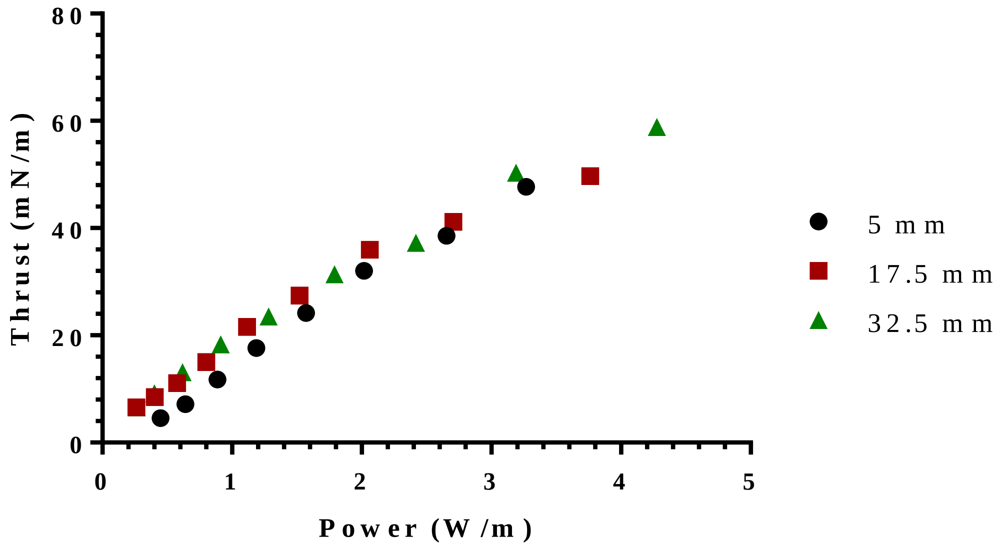

Figure 43 Thrust vs power (T-P) at 120mm separation

The most promising research on collector electrode enhancement was conducted Masuyama and Barrett [24]by adding an intermediary grounded electrode between the emitter and collector. This novel geometrical scheme titled the dual thruster (DS), was believed to reduce the voltage charge on the collector electrode diminishing the production of opposite corona. As a result, increased thrust an efficiency where obtained whilst maintaining an efficient corona discharge.

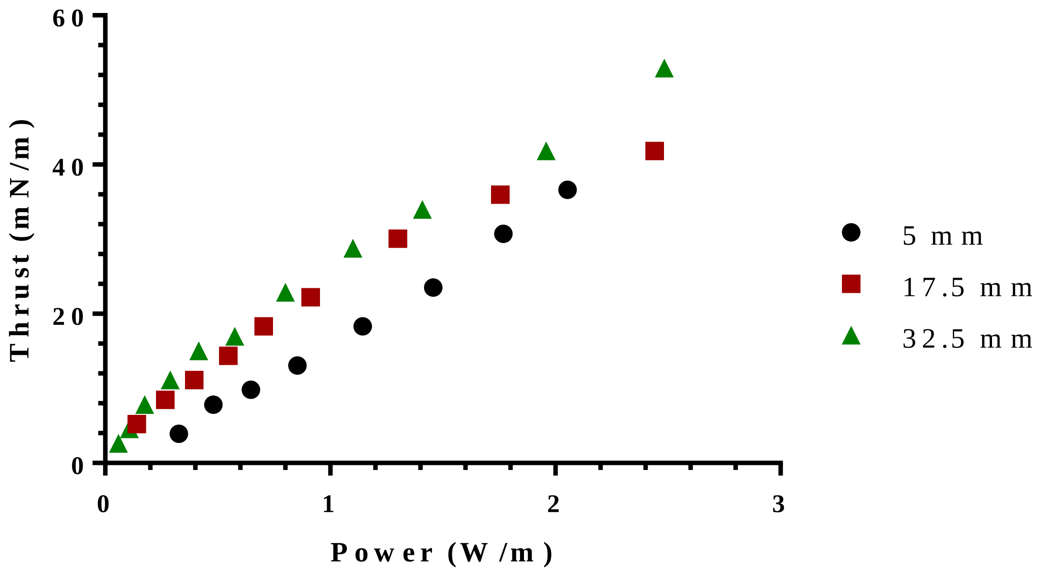

Figure 44 Thrust vs power (T-P) at 160mm separation

Rather than trying to enhance the emitter electrode and corona discharge properties which experience these maximums with respect to efficiency, research should aim to examine the electrostatic effect of the collector electrode. For this reason a set of cross examination experiments are conducted which vary the collector electrode radius of curvature r_c withinter electrode separation distance$d$ to gain an in depth understanding and achieve an enhancement of the physical parameters governing thrust and performance. To this end, three different collector electrode radius of curvature are examined on wire to aerofoil configurations against three separation gaps $r_c = 0.5mm, 17.5mm$ $32.5mm$ and $d = 20mm - 160mm$respectively. The emitter electrode diameter and collector electrode depth also remained $\emptyset_w = 0.1mm$ and $l_c = 40mm$ respectively.

Table 7 Ion mobility values for different r_c at different gaps

Electrode Separation (*mm*)	μ^+ $(\mathbf{10^{-4}m^2V^{-1}s^{-1}})$ $r_c = 0.5mm$	μ^+ $(\mathbf{10^{-4}m^2V^{-1}s^{-1}})$ $r_c = 17.5mm$	μ^+ $(\mathbf{10^{-4}m^2V^{-1}s^{-1}})$ $r_c = 32.5mm$
20	4.2	3.72	6.12
40	2.89	3.47	3.2
80	2.79	3.3	4.1
120	3.36	2.9	3.13
160	4	2.91	2.79

Figures 42, 43 and 44 outline the thrust to power (T-P) measurements of the collector electrode radii at 80mm, 120mm and 160mm respectively. Interestingly, we see that as the separation gap increases the thrust to power ratio of the larger electrode also increases with collector electrode size. At smaller separation gaps the smaller radius of curvature is more effective because there is the optimum trade-off between forces as expressed in equation 20. However, as the separation between electrode moves towards 160mm we observe that maximum thrust levels are obtained with a collector electrode with the largest radius of curvature $r_c = 32.5mm$.

Examining the ion mobility values in Table 7 which were interpolated from equation 15 we see that there is a progressive enhancement as aerofoil radiuses of curvature increases with inter electrode gap. It seems that the optimum electrode gap for $r_c = 0.5mm$ is between 40mm and 80mm as the ion mobility is lowest between these separations. For $r_c = 17.5mm$ the optimum region lies between 80mm and 120mm, making note that between $d = 120 - 160mm$ the mobility of ions remains relatively equal. Lastly, for $r_c = 32.5mm$ the optimum inter electrode gap is 120 to 160 and beyond.

Table 8 Constant C values for different r_c at different gaps

Electrode Separation (mm)	$\mathbf{C}(\mu \boldsymbol{AkV^{-2}m^{-1}})$ $r_c = 0.5mm$	$\mathbf{C}(\mu \boldsymbol{AkV^{-2}m^{-1}})$ $r_c = 17.5mm$	$\mathbf{C}(\mu \boldsymbol{AkV^{-2}m^{-1}})$ $r_c = 32.5mm$
20	7.303	7.4832	9.443
40	1.381	1.81	2.0491
80	0.3226	0.5366	0.6427
120	0.1252	0.1826	0.223
160	0.064	0.1186	0.1187

Table 8 outlays the constant *C* values for the different radii and different electrode gaps which were interpolated from equation 16. We see that for any given gap, the value of *C* remains relatively proportioned with respect to the aerofoil radius of curvature indicating the dominance of inter electrode separation on the constant *C*.

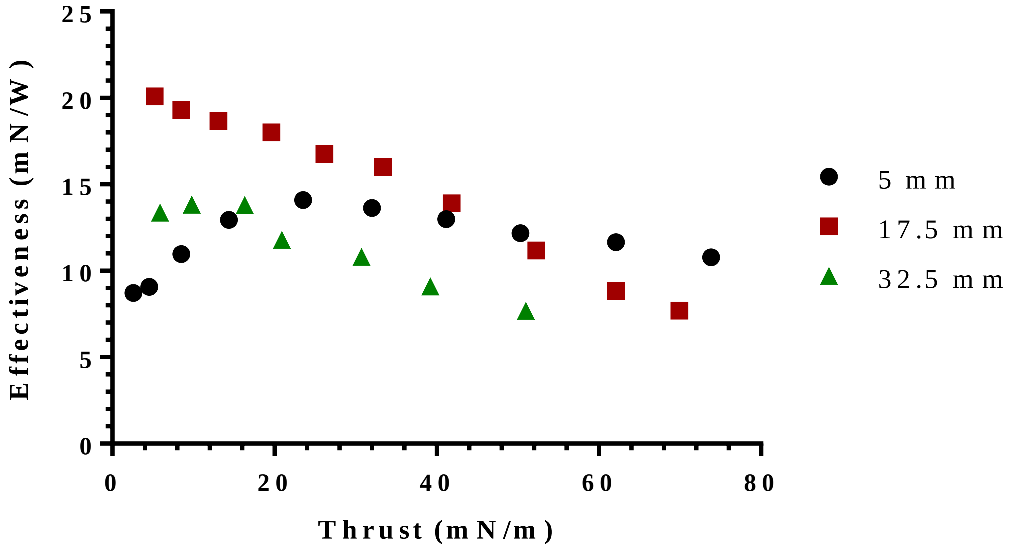

Figure 45 Effectiveness vs thrust (θ-T) at 80mm separation

From the effectiveness versus thrust measurements (θ-T) in Figures 45, 46 and 47 we see that the aerofoil with larger $r_c$grows moreefficient at increased separation gaps than a smaller r_c. A common trend becomes evident from the θ-T plots that the larger radii of curvature also have a superior effectiveness at lower thrusts than smaller radii across any separation gap. This may be attributed to the fact that the drag forces at smaller levels of thrust are negligible in comparison to the strength of the electrostatic forces as expressed in Section 3.4.5. Hence, we may conclude that equation 22 is only effective for smaller electrode gaps or higher thrusts at larger gaps.

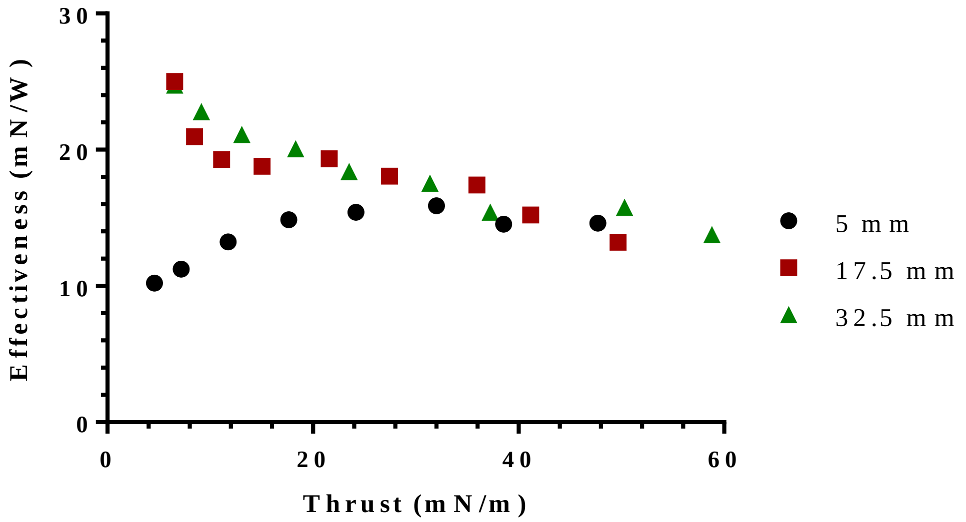

Figure 46 Effectiveness vs thrust (θ-T) at 120mm separation

Figure 47 displays θ-T at 80mm separation where the maximum effectiveness of $r_c = 0.5$ is $14mNW^{-1}$ and $r_c = 17.5mm$ is $20mNW^{-1}$ whereas the maximum effectiveness of $r_c = 32.5mm$ is $7mNW^{-1}$. Comparing these values to $160mm$ separation in Figure 47 we see that the smallest radius of curvature makes only a slight increase in its average effectiveness. Figure 48 displays a comparison between $r_c = 17.5mm$ and $r_c = 32.5mm$ at $d = 80mm$ and $d = 160mm$. Immediately, we see that $r_c = 32.5mm$ surpasses $r_c = 17.5mm$ with electrode separation a maximum of $\theta = 44.5mNW^{-1}$ at $2.615mNm^{-1}$ of thrust. This is an enhancement of $30.7mNW^{-1}$ from $d = 80mm$ whereas $r_c = 17.5mm$ only makes an improvement of $17.2mNW^{-1}$ between the two electrode separations. This same trend is observed for $r_c = 5mm$ and $r_c = 17.5mm$ between $d = 20mm$ and $d = 120mm$ (Appendix B).

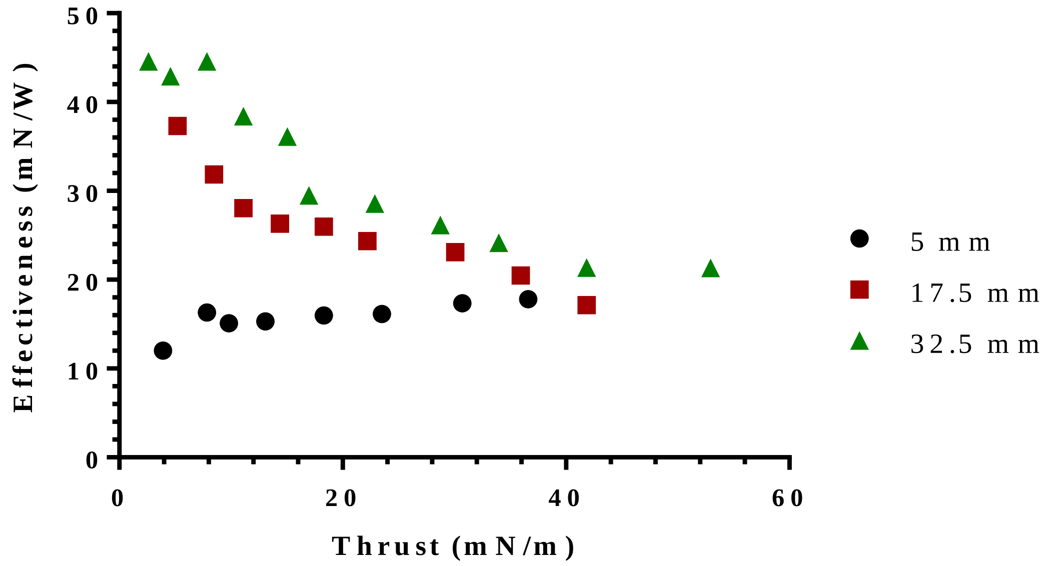

Figure 47 Effectiveness vs thrust (θ-T) at 160mm separation gap

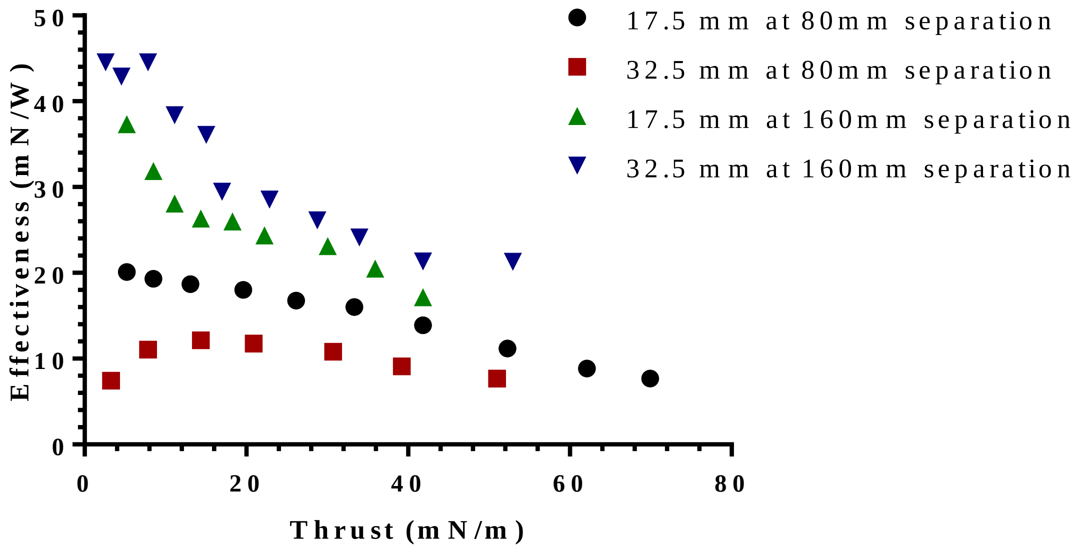

Figure 48 Effectiveness vs Thrust (θ-T) for curvature and separation

Hence, we may draw some conclusions on the cross examining of r_c with inter-electrode separation *d:*

- Firstly, we notice that as the separation gap increases, the effectiveness for collector electrodes with larger r_c also increases. Correspondingly, small r_c has a decreased effectiveness at larger gaps and low thrust. Hence, we can conclude that the most effective EHD model involves a large aerofoil radius of curvature with large separation gap at low thrust.

- We also notice that at larger gaps the thrust to power ratio is higher for larger $r_{c.}$ Although the trade-off between surface area and electrostatic force on large electrode is significant at smaller gaps, we see at larger gaps that the obstruction of neutral air flow by the larger electrode diminishes with respect to separation gap. Hence, the dominant electrostatic forces results in increased net thrust.

- The current to voltage readings show that as the separation gap increases the larger r_c obtains a higher current to voltage reading. This is expected since the larger r_c has a larger surface area for ions to engage resulting in a higher current reading. At smaller gaps the current readings are relatively similar.

- We notice that the lower end effectiveness of smaller diameters is very low. Larger diameters are very effective. This may be attributed to the fact that at low power levels the wind velocity is minimal. Hence, the larger diameter collector electrodes have maximum electrostatic influence with minimal drag reduction.

Chapter 4 SOLID DIELECTRIC EXPERIMENTS

This chapter outlines and discusses a series of experiments aimed at understanding and further enhancing thrust levels and efficiency. These experiments are conducted in accordance with the original claims of Thomas Townsend Brown which involves highly charged electrodes separated by solid dielectric materials.

4.1 INTRODUCTION

A key factor to the anomalous force between charged plates, and the reason for such controversy surrounding the effect explanation is due to the fact that several experiments [27, 29, 33] have shown that ionization of a fluid dielectric is not a necessary parameter for thrust. This result would invalidate ion wind as the sole cause of thrust to all the claims of Brown. Consequently, the following experimental investigation deals with plates which are charged to high voltages that attempt to avoid any ionic wind creation. These experiments are based on the observations of Brown in his 1928[8] and 1960[10] patents which involve the use of solid dielectric materials. Although previously, the effect was observed with air acting as the dielectric material separating the electrodes; it is known to function with solid dielectrics insulated from any fluid medium. The effect is believed to increase with an increase in the distortion of the electric field which can be achieved through optimisation of certain variables. Brown outlined these observations in his 1960 paper. Alongside the work of Buehler[29] we may come to several new conclusions constituting the effect which include:

1. The effect moves in the direction of the positive plate, irrespective of its direction with the earth's surface.

2. The effect, when shielded in a faraday cage produces no thrust. This shows that it depends on the earth electric field despite being independent of it as in point 1.

3. The observed thrust increases with a varying electric field, preferably in the direction of the positive pole. This may be achieved by varying the dielectric

material based on strength or permittivity, varying the dimensions of the electrodes, creating different layers of the dielectric material or by changing the dielectric shape.

Surprisingly, very little experimental research other than those elaborated on in section 2.1.3exists on the observed force with charged plates and solid dielectric materials. Although Brown mentions several ways to increase thrust, there is very little published material to verify his observations. To this end, and to fulfil the aims of this thesis, the following chapter intends to reproduce some of the experiments outlined by Brown to accept or reject these claims and move closer to an in depth understanding of the Biefeld-Brown effect.

4.2 EXPERIMENTAL SETUP

Experiments are conducted under similar conditions to the fluid dielectric experiments in Chapter 3 i.e. the temperature was maintained at $20^{\circ}C$ and the relative humidity was maintained at 60%. The electrode plates used for experimentation consist of copper sheets with areas$A = 150mm\ x\ 150mm$and $A = 300mm\ x\ 300mm$ and thickness of $\delta = 0.15mm$. Sheets were tested as single plates, parallel capacitor units as shown in the Figure 53 and as asymmetric capacitor units. All tests were conducted under high DC voltage and changes in mass of the plates were determined on an electronic scale with $\pm 0.01g$ precision. Further tests involved the use of right angle glass prisms shown in Figure 49 made from Borosilicate Crown glass (Optical N-BK7) with a dielectric constant of $k = 4.87$. The prism was a right angled triangle with side length of $l_s = 40mm$and depth $d_p = 20mm$. The glass prisms were used to conduct experiments which alter the shape and mass of dielectric material separating the copper electrode plates. In addition the edges of the copper plates were covered with a high voltage insulating material to prevent any corona discharge forming on the outer boundaries which would impair results.

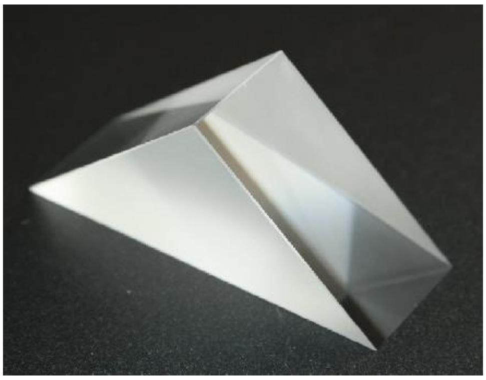

Figure 49 Dielectric material used for experiments (N-BK7)

4.3 PROOF OF CONCEPT

4.3.1 Single Plate

The aim of this experiment is to show that a conducting material experiences a reduction in weight with respect to the earth's surface when charged to high voltage. In this particular case a section of copper sheet $A = 150mm\ x\ 150mm$ and $A = 300mm\ x\ 300mm$both withthickness $\delta = 0.15mm$are charged in $2kV$ iterations with their thrust measured.

Figure 50represents the thrust versus voltage plot (V-I) where we see that the positively charged plates thrust is proportional to square of voltage. In addition, we notice that there is a consistant enhancement in the thrust to voltage ratio between the two plate sizes.

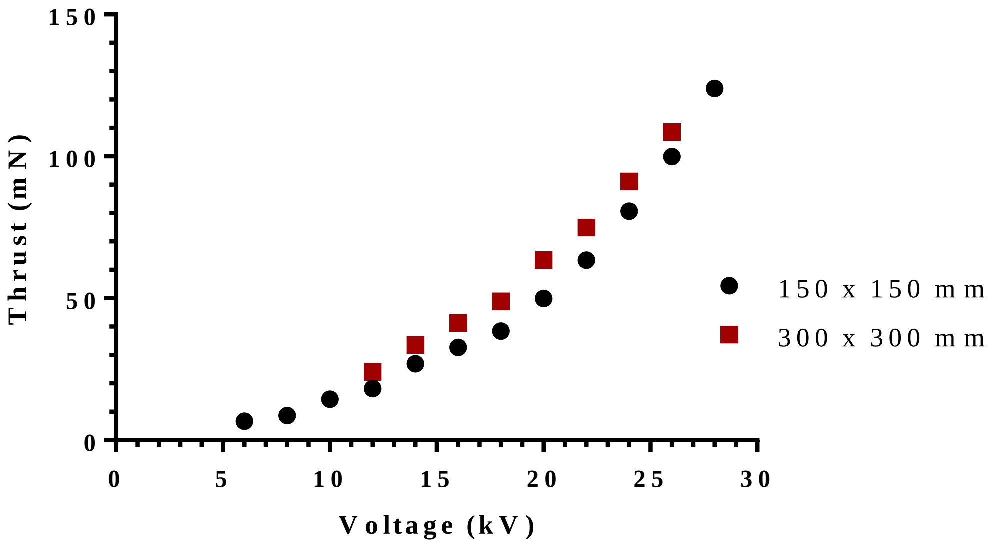

Figure 50 Thrust versus Voltage on charged single plate

As a result, we draw two conclusions from this experiment, firstly, these experiments immediately indicate that the force on charged electrodes is not the effect of ionic wind and EHD forces but is due to aphenomenon yet unknown; secondly, the force on charged plates is proportional to the surface area of the electrodes such that there is a consistent increase in thrust. This experiment adds evidence to the torque pendulum experiments of Saxl [26] and also to the single charged plate experiments conducted by Buehler [29] and Bahder and Fazi [9].

4.3.2 Parallel Plates

This next experiment aims to determine the effect of charged parallel plates and how the distance between these plates affects the observed thrust. By changing the distance between the plates, the capacitance of the system is altered. This will provide insight into the relationship between the stored energy within the plates and observed thrust levels.

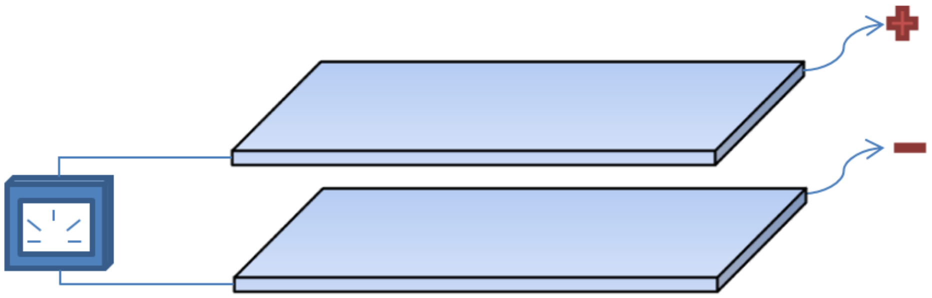

Figure 51 Basic outline of experimental rig of parallel plate capacitor

Figure 52 outlines the thrust to voltage measurements for electrode gaps ranging from 2mm-14mm with air dielectric. The results indicate that there is a direct correlation between the distance of the electrodes and thrust to voltage performance such that $T \propto {}^{1}/_{d}$.

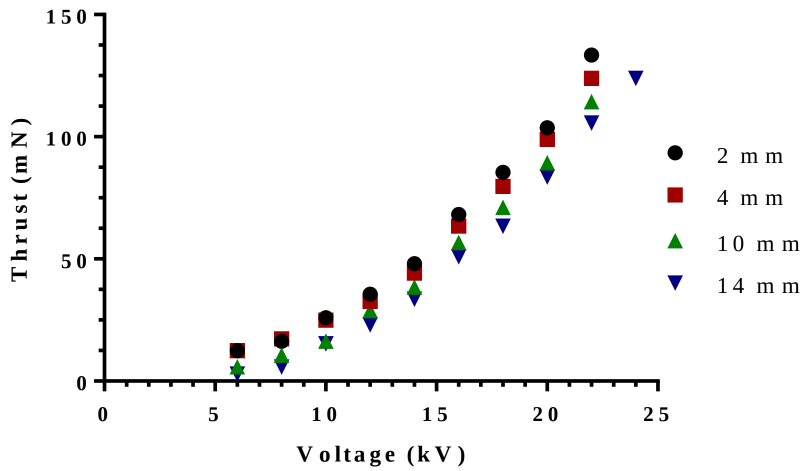

Figure 52 Thrust versus voltage for parallel plates

4.4 SOLID DIELECTRIC EXPERIMENTS

4.4.1 Dielectric Mass

The next experiment examines the effect of a solid dielectric material between the copper electrode plates. To this end, we aim to determine a relationship between the mass of dielectric material separating the electrodes and thrust levels. The electrodes used consist of $A = 150mm\ x\ 150mm$ copper plates with thickness $\delta = 0.076mm$. The separating dielectric consisted of the Optical BK7 glass with mass $m = 30g$. The thrust was measured with one and two sections of Optical N-BK7 glass to make comparisons.

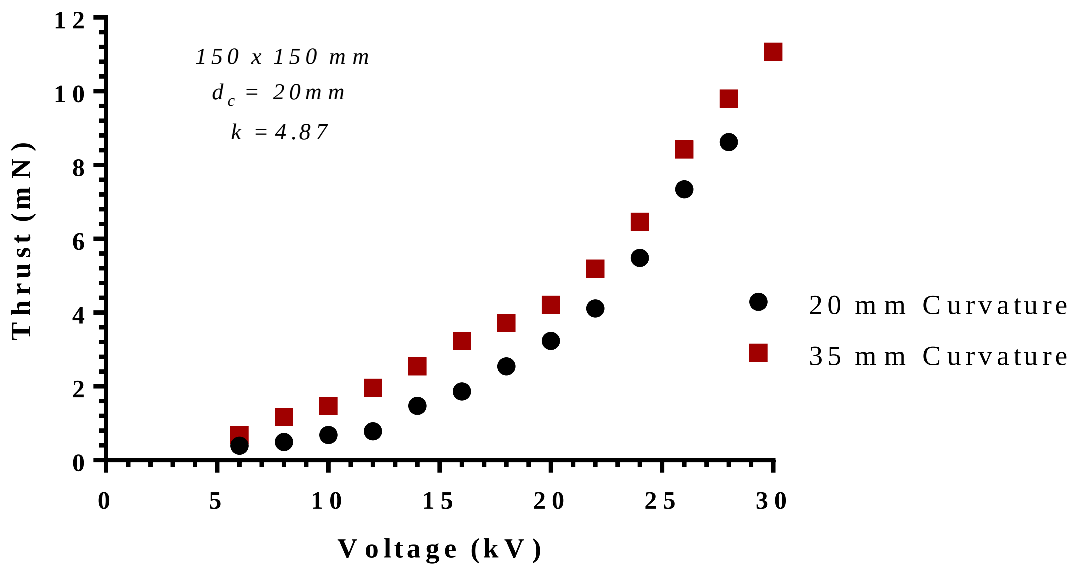

Figure 53 Thrust versus voltage for dielectric mass

Figure 53 provides the thrust versus voltage (T-V) measurements for a single mass block and double mass block respectively. Again, we observe that the thrust to voltage ratio is directly proportional to the amount dielectric material between the plates as well as the materials dielectric strength.

From the above proof of concept experiments, we may conclude that the force observed on charged plates is directly related to the capacitance of the system such that

$$C = \varepsilon_r \varepsilon_0 \frac{A}{d_c} \tag{27}$$

Where ε_r is dielectric constant between the plates and ε_0 is the electric constant $\varepsilon_0 = 8.854 \times 10^{-12} Fm^{-1}$, A is the area of the plates andd_c is the distance between them. These observations are consistent with those of Buehler[29] who deduced from his experimental research that parallel plates demonstrate a linear relationship between the charging energy and observed thrust between the parallel plates. This energy relationship is expressed

$$F \cong kU \tag{28}$$

Where $k \cong 0.47NJ^{-1}$ and U is then energy of the capacitor related to equation 27.

4.4.2 Dielectric Mass Distribution

It has been shown through the previous experiments that the observed thrust on parallel plate capacitors is a function of the energy stored within the system. However, it was expressed by Brown and others [44, 45] that thrust may be enhanced also by maximising the distortion of the electric field between the charged electrodes. For this reason aim of this experiment is to verify these claims and enhance the observed thrust on charged electrodes. To this end, an experiment is conducted which aims to understand how the distribution of the dielectric material affects the observed levels of thrust. The triangular glass prisms used in section 4.4.3 are used again between the capacitor system whose plates consist of an area $A = 150mm\ x\ 150mm$, however they are now set so that they constitute an unequal mass distribution. From this, a distortion to the electric field is obtained between the electrodes as proposed by Brown to enhance thrust. Additionally, this experiment aims to understand in which direction the mass distribution is most effective by facing the glass prims both upwards and downwards as shown in Figure 54.

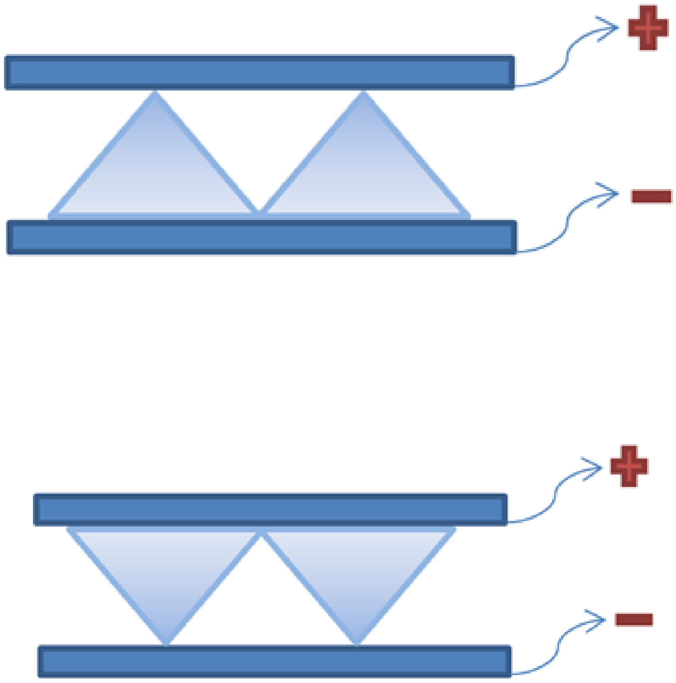

Figure 54 Experimental Setup of dielectric mass orientation

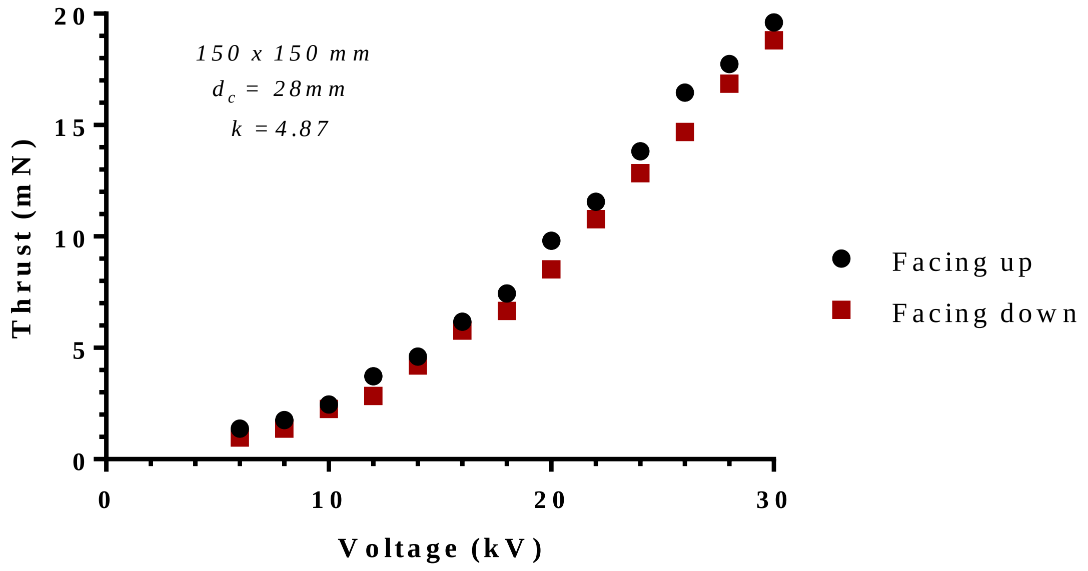

Figure 55 Thrust versus voltage of different dielectric mass orientation

Results shown in Figure 55 indicate that the distribution of dielectric mass is a function of the observed thrust. The results outline that the distribution of mass should decrease towards the electrode away from the earth's surface for enhanced results.

4.4.3 Origin of Force

An interesting aspect of the thrust observed on charged plates is that it does not seem to be the result of any reactionary force as outlined in Newtons third Law. There is no expulsion of material or wind from the system to warrant a reduction in weight of the system. At this point the thrust on charged plates appears to be in extreme violation of momentum and conservation [46]. Therefore, the following experiment aims to measure the reduction in weight of both the charged plates and the separating dielectric material individually. By understanding where the thrust is generated may provide greater insight into the workings of the system. Figure 56 outlines the experimental setup whereby the electronic balance is placed on the dielectric material as opposed to the capacitor plates.

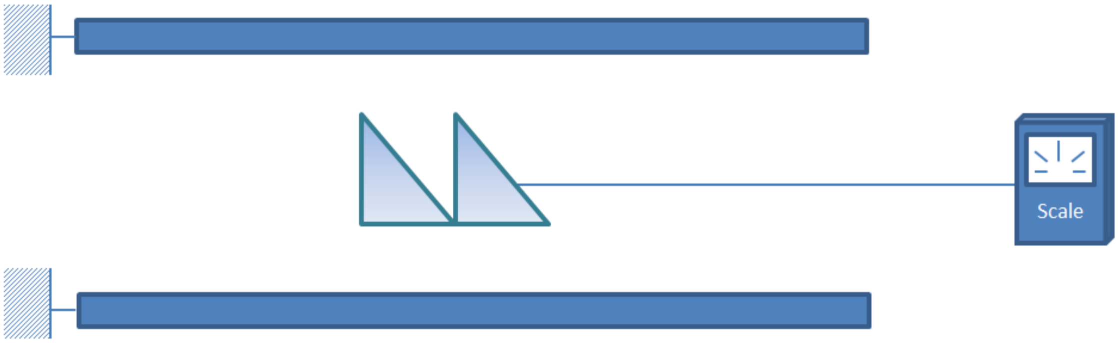

Figure 56 Experimental rig used to measure the thrust of dielectric material

Interestingly the experiment exhibits a measurement on the dielectric material and electrodes of exact proportion. There seems to be a force imparted onto the dielectric material by the charging of the plates which is reciprocated. If one of the constituents is held firmly the resultant force is observed on the other and vice versa. Hence, we may deduce that there is a direct relationship between the force imparted on the electrodes and the force on the dielectric.

Chapter 5 DISCUSSIONS

This chapter summarises the observations made in Chapters 2, 3 and 4 and discusses the results.

The research conducted in this thesis was an experimental investigation into the enigma of the Biefeld-Brown effect. This research was to be conducted with two primary objectives of investigation; firstly, an analysis of contradicting theories surrounding the effect that have resulted in ambiguity into the nature of observed thrust. Once this was achieved it was the second objective of this investigation to characterise the force on charged electrodes for enhanced performance and efficiency.

As was expressed in the literature review, a great schism eventuated for a possible explanation of the Biefeld-Brown effect. Since the discoveries by Brown which were expressed in his patents, an abundance of research has followed in an attempt to explain the anomalous force on charged electrodes. One school of thought proposes that the sole cause of thrust on the charged electrodes is due to the ionization of a fluid dielectric medium which in turn generates ions that are attracted electrostatically to the opposite electrode. In the process of this attraction, they collide with neutral air particles, thereby, generating thrust. Several researches[9, 20] have performed tests in vacuum chambers to further the proposal of the theory.

The second school of thought believes that ion wind effects cannot be the sole explanation to the thrust. Although no explanation has been provided for the null thrust in vacuum chamber tests, several experiments show that there is some electrostatic relationship with the earth's electric field which is not consistent with EHD theory. In addition, it has been shown that the presence of solid dielectric material between the charged electrodes enhances performance. Despite the extremely scarce published experimental research proposing these observations, it generates a strong case.

From the patents of Brown and through the literature up to date, one simple characteristic has stood out which seems to be a defining factor to understanding the Biefeld-Brown effect; some experiments utilise and require a fluid dielectric medium to function, whilst others, require only electric field shaping characteristics or solid dielectrics to store charge. For this reason, the experimental investigation conducted in this thesis was separated into two sections; chapter 3 investigated extremely asymmetric electrodes in a fluid dielectric i.e. air, whereas chapter 4 investigated the charging of parallel copper electrode plates separated by solid dielectrics.

The first of these phenomena discussed in this thesis involved the charging of electrodes of extremely asymmetrical dimensions in a dielectric fluid medium for the purpose of producing a corona discharge. This concept has developed to become known as the field of electro-hydrodynamics whereby thrust is generated when a positive corona discharge generated around an emitter electrode attracts electrostatically a larger collector electrode. A theoretical model for EHD thrust was provided in Section 3.2 which was correlated with the experimental results. The experimental investigation aimed to test the fundamental geometrical variables on a wire to aerofoil thruster utilising a positive corona. Beginning with a proof of concept case it was shown first and foremost that the force observed on extremely asymmetric electrodes was the result of ion wind. Experimental results matched well with the theoretical model to solidify the theory as the origin of thrust. The proof of concept case began with $T_{MAX} = 53mNm^{-1}$ at $10W$ of power and effectiveness$\theta = 18.84mNW^{-1}$ at $1.96mNm^{-1}$ of thrust. These results correlated well with results of others in literature. The experimental program from this point aimed to investigate further into the parameters of the wire to aerofoil configuration for enhanced performance and effectiveness. Firstly, it was shown that emitter electrode diameter had a major effect on the constant *C* and ion mobility μ^+ such that smaller diameters resulted in increased thrust and effectiveness. Consequently, it was deduced that the primary function of the emitter electrode is the ionization of the surrounding dielectric medium and was therefore preferred to be of minimal diameter. The following experiment investigated the effect of inter electrode gap ranging $d = 20mm - 160mm$ which concluded that as the separation between electrodes increased, there was an enhanced thrust to power curve (T-I). In saying this, we managed to achieve a maximum of $\theta = 37.3NkW^{-1}$ and $5.23mNm^{-1}$of thrust. Once the emitter electrode and separation gap had been characterized it was time to examine the collector electrode. To this end, tests were conducted on aerofoil depthl_c and radius of curvature r_c. It was observed that the foil depth did not have a major impact on the performance of the EHD model with thrust and effectiveness levels increasing slightly with depth. Radius of curvature experiments showed that large radii performed better at low thrusts where wind velocity was low. However, it was shown that that was a trade-off between the obstruction to neutral air flow and the electrostatic force of the collector electrode.

The last of the characterization experiments was aimed to characterize the direction and velocity of air flow around the wire to aerofoil configuration. Through the smoke and flame tests it was observed that the ion wind moved towards the corona discharge and then down the surface of the collector electrode. Hence, different collector electrode shapes were examined for performance enhancement purposes. It was shown that from the experiment that although some geometry produced the highest wind flow, they did not produce the highest thrust. This was because the wind flow was disturbed by the cross section of the collector electrode. It was concluded that the optimum geometry for EHD thrusters was in fact the wire to aerofoil configuration.

These are the experiments which constituted characterizing EHD thrusters. Following this characterization an experiment was conducted which sought the influence of magnetic fields on the observed thrust. It was shown that the introduction of a permanent magnet whose field coincided with the corona discharge region resulted in enhanced thrust. A consistent enhancement of thrust was observed directly proportional to the voltage input indicating a direct enhancement. Lastly, cross examination experiments was conducted between aerofoil radiuses of curvature and inter electrode separation. It has been shown in this experiment that a direct relationship exits, whereby increased thrust and effectiveness are a function of increased radius of curvature and separation. To this end, utilising a radius of curvature of $32.5mm$ resulted in $13.8mNW^{-1}$increase over $17.5mm$ at a separation of $160mm$. It was therefore concluded that a direct relationship exists between the collector electrode radius of curvature and inter-electrode separation distance such that $d \propto r_c$.

The second phenomena discovered by Brown was outlined in patents issued in1928[8] and 1965[12]which describes the effect on charged plates that do not involve the ionization of the surrounding medium. This 'alternate' Biefeld-Brown effect is yet to be explained or even attributed to a particular field of physics.

From the experimental program in Chapter 4 we initially notice that the charging of a single plate experiences a thrust force away from the earth's surface. This initial test also acted as the proof of concept experiment which indicates that the force on charged plates is not a result of ion wind theory or the generation of a corona discharge. Secondly, we see that the observed thrust is directly related to the capacitance or energy of the system i.e. the ability for the system to store charge results in a direct correlation with thrust performance. This observation has been confirmed by literature [27, 29] whereby $T \propto C$. Hence, factors including the dielectric constant of material separating the plates, area of the plates and distance between the plates all have a direct and proportional impact on the observed thrust.

The third result indicates that the distribution of this energy storage also impacts the thrust such that an increase in the capacitance towards the earth's surface enhances thrust levels. This was shown in experiments where the observed thrust was measured with a dielectric material facing both towards and away from the earth. From this it may be concluded that the magnitude of distortion of the electric field is a factor in the observed thrust. Lastly, it is shown in the origin of force experiment that there is a direct relationship between the force on the charged electrodes and the force on the intermediate dielectric mass. The electric field of the system seems to apply a force onto the dielectric material between the plates. In return, the dielectric material reacts to this force with an equal and opposite reaction which results in a mechanical thrust on the entire system.

Hence, as a deduction of the experimental results we conclude that the mechanism behind the observed thrust is dependent on the polarization of the dielectric material separating the electrodes. The force on charged electrodes may be analogous to the compression of a spring, whereby the potential energy stored in the spring results in a desire return to its natural position. Albeit, the electric field generated by the charging of the plates acts as this source of energy which is stored in dielectric material. As a result, the dielectric is ‘stretched’ in a dielectrophoretic process [47]. So long as the electric field exists, the dielectric material will exhibit a force back onto the electrodes. This explains why no force has been observed in vacuum chambers. However, no explanation may be made yet as to the unidirectional movement away from the earth’s surface.

Essentially, it is concluded that the mysterious Biefeld-Brown effect has been misunderstood and confused amongst most of the researchers today. By studying the patents of Brown as well as conducting a series of experiments which mimic those in the patents we have shown that the Biefeld-Brown effect consists of two completely individual phenomena.

Chapter 6 CONCLUSIONS

This chapter summarises the conclusions made in this research.

This thesis investigated the anomalous force on charged electrodes, namely, the Biefeld-Brown effect. A detailed investigation into the available literature coupled with an experimental program has successfully fulfilled the primary research objectives outlined in section 1.2. The work of Thomas Townsend Brown between the 1920's and 1960's consisted of two independent lines of research which have been confused for decades. One line of research involved the ionization of a fluid dielectric medium between extremely asymmetric electrodes. The other line of research was the anomalous force on charged electrodes which did not involve any corona discharge effects. An experimental program was conducted to investigate each of these phenomena individually for the purpose of validating and enhancing their performance.

6.1 FLUID DIELECTRIC CONCLUSIONS

The main conclusions from the experimental investigation into extremely asymmetric electrodes in a fluid dielectric medium are summarised below:

- Firstly, the force observed on the electrodes correlates well with the 1-D electro-hydrodynamic (EHD) theoretical model validating ion wind as the proper explanation for the effect.

- Secondly, it was shown the thrust performance and efficiency levels enhanced when emitter electrode diameter ϕ_w was minimised and inter electrode separation d was increased.

- Thirdly, it was shown that the introduction of magnetic fields enhanced thrust performance which was proportional to voltage input.

- Lastly, cross examining the collector electrode radius of curvature with the inter-electrode separation displayed a relationship whereby thrust and efficiency are enhanced when the radius of curvature r_c increased proportionally with electrode separation d.

6.2 SOLID DIELECTRIC CONCLUSIONS

The main conclusions from the experimental investigation into charged electrodes that do not require the effects of corona discharge are summarised below:

- Firstly, the effect was observed to move away from the upwards in all cases.

- Secondly, it was evident that the thrust on charged the charged plates was a function of the energy stored in the system such that area of the plates *A*, dielectric material mass and its strength *k* and the distance between the plates *d* were all factors.

- Lastly, it was shown that the ability for the electric field to be distorted impacted the observed effect. This was shown by placing more dielectric mass near one electrode to enhance thrust.

6.3 FUTURE WORK

The findings and conclusions drawn from this thesis have contributed towards a brighter and promising future for electric propulsion through charged electrodes. A fully developed craft utilising this technology will be without the limitations and carbon footprint of conventional propulsion systems today. Future recommendations for research into charged electrodes for propulsion should begin comparing experimental data with numerical simulation for a more in depth understanding of the propulsive capabilities. Secondly, a study of the potential energy stored in the separating dielectric material is required for a deeper understanding of the relationship between electricity and its effect on matter. It is this relationship which will form the basis of future electric propulsion craft.

REFERENCES

[1] Tajmar M. Biefeld-Brown effect: Misinterpretation of corona wind phenomena. AIAA journal. 2004;42:315-8.

[2] Loder III TC. Implications of Outside-the-Box Technologies on Future Space Exploration and Colonization. Expanding the Frontiers of Space. 2003;654:1199-203.

[3] Ianconescu R, Sohar D, Mudrik M. An analysis of the Brown–Biefeld effect. Journal of Electrostatics. 2011;69:512-21.

[4] Tajmar M. Experimental investigation of 5-D divergent currents as a gravity-electromagnetism coupling concept. SPACE TECHNOLOGY AND APPLICATIONS INTERNATIONAL FORUM-2000. Vol. 504: AIP Publishing; 2000. p. 998-1003.

[5] Musha T. Connection Between Einstein's Unified Field Theory and the Biefeld-Brown Effect.

[6] Musha T. Missions to the outer solar system and beyond.

[7] Maknickas AA. Biefeld-Brown effect and space curvature of electromagnetic field. 2013.

[8] Brown TT. A Method of and an Apparatus or Machine for Producing Force or Motion. GB Patent. 1928;300.

[9] Bahder TB, Fazi C. Force on an asymmetric capacitor. arXiv preprint physics/0211001. 2002.

[10] Brown TT. Electrokinetic apparatus. Google Patents; 1960.

[11] Brown TT. Electrokinetic transducer. Google Patents; 1962.

[12] BROWN T. BROWN ELECTROKINETIC APPARATUS. Google Patents; 1965.

[13] Fantel H. Major de Seversky's Ion Propelled Aircraft. Popular Mechanics August. 1964.

[14] Pekker L, Young M. Model of ideal electrohydrodynamic thruster. Journal of Propulsion and Power. 2011;27:786-92.

[15] DE A. Ionocraft. Google Patents; 1964.

[16] Cheng S-I. Glow discharge as an advanced propulsion device. ARS Journal. 1962;32:1910-6.

[17] Christenson EA, Moller PS. Ion-neutral propulsion in atmospheric media. AIAA Journal. 1967;5:1768-73.

[18] Robinson M. Movement of air in the electric wind of the corona discharge. American Institute of Electrical Engineers, Part I: Communication and Electronics, Transactions of the. 1961;80:143-50.

[19] Bondar H, Bastien F. Effect of neutral fluid velocity on direct conversion from electrical to fluid kinetic energy in an electro-fluid-dynamics (EFD) device. Journal of Physics D: Applied Physics. 1986;19:1657.

[20] Talley RL. 21st Century Propulsion Concept. DTIC Document; 1988.

[21] Primas J, Malík M, Jašíková D, Kopecký V. Force on a High Voltage Capacitor with Asymmetrical Electrodes. Proceedings of WASET 2010 Conference, Amsterdam: Citeseer; 2010. p. 335-9.

[22] Canning FX, Melcher C, Winet E. Asymmetrical capacitors for propulsion. NASA TM CR-2004-213312. 2004.

[23] Wilson J, Perkins HD, Thompson WK. An investigation of ionic wind propulsion. 2009.

[24] Masuyama K, Barrett SR. On the performance of electrohydrodynamic.

[25] Ieta A, Ellis R, Citro D, Chirita M, D'Antonio J. Characterization of Corona Wind in a Modular Electrode Configuration. Proc ESA Annual Meeting on Electrostatics2013. p. 1.

[26] Saxl EJ. An electrically charged torque pendulum. Nature. 1964;203:136-8.

[27] Stephenson GV. The Biefeld Brown Effect and the Global Electric Circuit. SPACE TECHNOLOGY AND APPLICATIONS INT FORUM-STAIF 2005: Conf Thermophys in Micrograv; Conf Comm/Civil Next Gen Space Transp; 22nd Symp Space Nucl Powr Propuls; Conf Human/Robotic Techn Nat'l Vision Space Expl; 3rd Symp Space Colon; 2nd Symp New Frontiers. Vol. 746: AIP Publishing; 2005. p. 1249-55.

[28] Liu Y-c, Yang X-s, Guan T-r, Hu E-k, Wang G-z, Huang Z-f. Test of Saxl's effect: No evidence for new interactions. Physics Letters A. 1998;244:1-3.

[29] Buehler DR. Exploratory research on the phenomenon of the movement of high voltage capacitors. Journal of Space Mixing. 2004;2:1-22.

[30] Holzworth R. Quasistatic electromagnetic phenomena in the atmosphere and ionosphere, Handbook of Atmospheric Electrodynamics, I. Hans Volland I. 1995:235-66.

[31] Matsoukas G, Ahmed N. Experimental investigation of employing asymmetrical electrodes in propulsion of vehicles. Procedia Engineering. 2012;49:247-53.

[32] Loeb LB. Fundamental processes of electrical discharge in gases: John Wiley & Sons; 1939.

[33] Musha T. Theoretical explanation of the Biefeld Theoretical explanation of the Biefeld-Brown Effect Brown Effect Brown Effect.

[34] Musha T, Minami Y. Field Propulsion System for Space Travel. Bentham Books; 2011.

[35] Cameron J. Asymetric gravitational wave propulsion system. Google Patents; 2001.

[36] Dröscher W, Häuser J. Space Propulsion Device. 2004.

[37] Townsend J. The theory of ionization of gases by collision: D. Van Nostrand Company; 1910.

[38] Malík M, Primas J, Kopecký V, Svoboda M. Calculation and measurement of a neutral air flow velocity impacting a high voltage capacitor with asymmetrical electrodes. AIP Advances. 2014;4:7137.

[39] Kiousis KN, Moronis AX, Fruh WG. Electro-Hydrodynamic (EHD) Thrust Analysis in Wire-Cylinder Electrode Arrangement. Plasma Science and Technology. 2014;16:363.

[40] Chung CF, Li WJ. Experimental studies and parametric modeling of ionic flyers. Advanced intelligent mechatronics, 2007 IEEE/ASME international conference on: IEEE; 2007. p. 1-6.

[41] Moreau E, Benard N, Lan-Sun-Luk J-D, Chabriat J-P. Electrohydrodynamic force produced by a wire-to-cylinder dc corona discharge in air at atmospheric pressure. Journal of Physics D: Applied Physics. 2013;46:475204.

[42] Serway R, Jewett J. Physics for scientists and engineers: Cengage Learning; 2013.

[43] Martins AA, Pinheiro MJ. On the influence that the ground electrode diameter has in the propulsion efficiency of an asymmetric capacitor in nitrogen gas. Physics of Plasmas (1994-present). 2011;18:033512.

[44] BAHNSON. Google Patents; 1960.

[45] Bahnson AH. Electrical thrust producing device. Google Patents; 1966.

[46] Woodward JF. “Breakthrough” Propulsion and the Foundations of Physics. Foundations of Physics Letters. 2003;16:25-40.

[47] Matsoukas G, Ahmed N. Investigation of Ionic Wind as a Means of Generating Propulsive Force. International Review of Aerospace Engineering. 2012;5.

APPENDIX A

Wire diameters:

Wire diameter (mm)	C	CV_o	V_o
0.11	1.81	12.6	6.961326
0.5	1.615	13.4	8.297214
1	1.0427	9.7012	9.303923
1.25	0.9907	10.068	10.16251

Wire Diameter	F/I	$\frac{F}{I}\cdot 10^3$	μ
0.11	0.1154	115.4	0.000347
0.5	0.0918	91.8	0.000436
1	0.083	83	0.000482
1.25	0.0764	76.4	0.000524

Separation gaps:

Seperation Distance (mm)	C	CV_o	V_o
20	7.4832	42.013	5.614309
40	1.81	12.6	6.961326
60	0.8289	6.2639	7.556883
80	0.5366	4.2511	7.922288
120	0.1826	1.5619	8.553669
160	0.1186	1.0401	8.769815

Seperation Distance (mm)	F/I	$\frac{F}{I} \cdot 10^3$	μ
20	0.0537	53.7	0.000372
40	0.1154	115.4	0.000347
60	0.1896	189.6	0.000316
80	0.2423	242.3	0.00033
120	0.4135	413.5	0.00029
160	0.55	550	0.000291

APPENDIX B

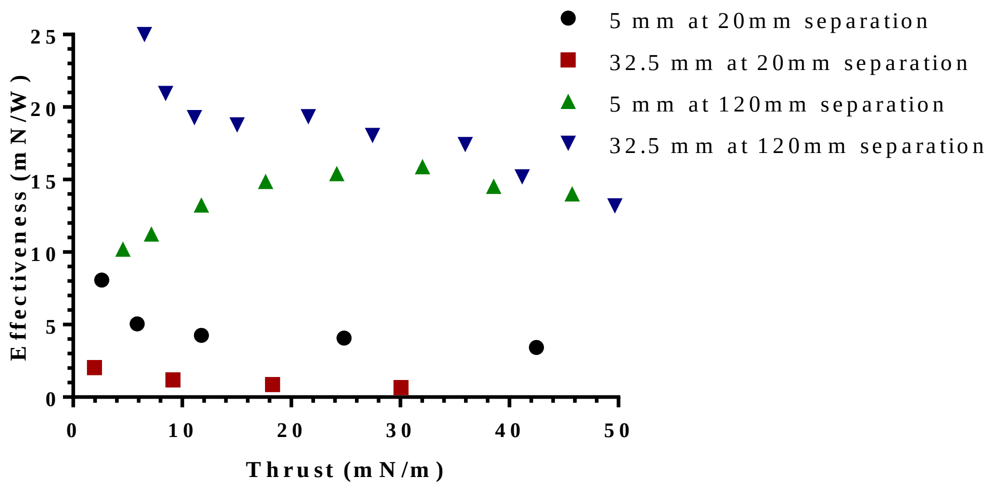

Figure 57 Effectiveness vs Thrust (θ-T) for curvature and separation